Metamorphism in the roots of mountain belts and its effect on rock technical properties

A case study of the Eastern Segment, Sveconorwegian orogen

Urueña, Cindy

2023

Document Version:
Publisher's PDF, also known as Version of record

LITHOLUND THESES 38

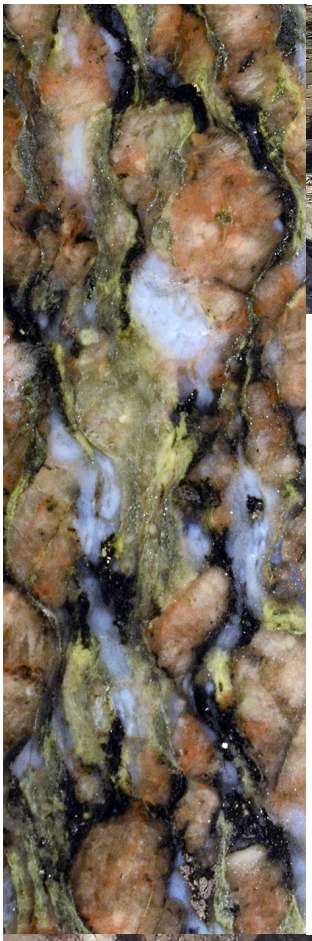

Metamorphism in the roots of mountain belts and its effect on rock technical properties – A case study of the Eastern Segment, Sveconorwegian orogen

CINDY LIZETH URUEÑA SUÁREZ
LITHOSPHERE AND BIOSPHERE SCIENCE | DEPARTMENT OF GEOLOGY | LUND UNIVERSITY 2023

Printed by Media-Tryck, Lund 2023 NORDIC SWAN ECOLABEL 3041 0903

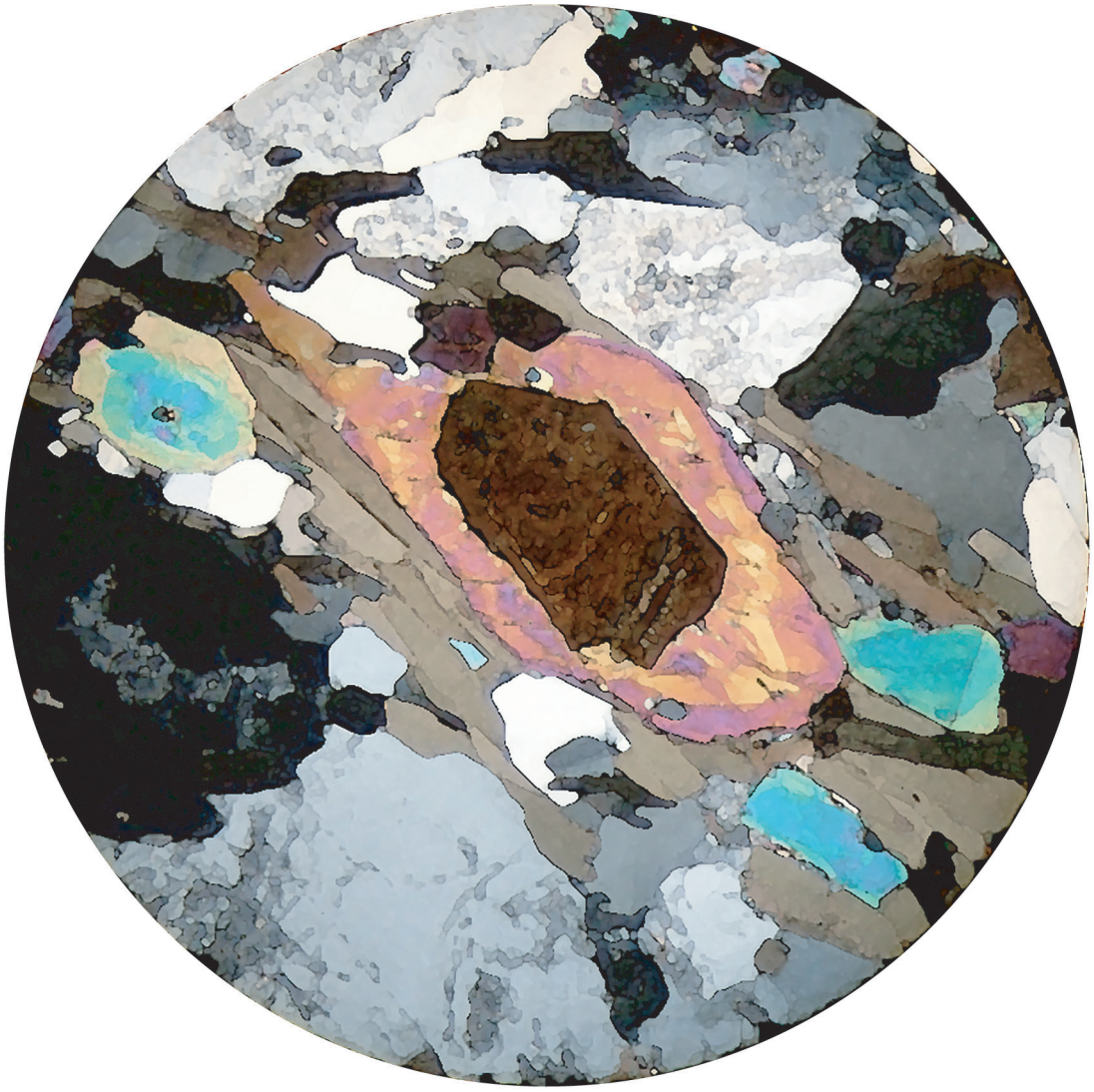

Metamorphic epidote with relict igneous allanite core (watercolor illustration)

LUND UNIVERSITY

Lithosphere and Biosphere Science
Department of Geology
Lund University
Sölvegatan 12
SE-223 62 Lund, Sweden
Telephone +46 46 222 78 80

ISSN 1651-6648
ISBN 978-91-87847-72-1

LITHOLUND THESES 38

Metamorphism in the roots of mountain belts and its effect on rock technical properties

A case study of the Eastern Segment, Sveconorwegian orogen

Cindy Lizeth Urueña Suárez

LUND
UNIVERSITY

Lithosphere and Biosphere Science
Department of Geology

DOCTORAL DISSERTATION
by due permission of the Faculty of Science, Lund University, Sweden.
To be defended at Pangea, Geocentrum II, Sölvegatan 12, on the 17th of May 2023 at 13.00.

Faculty opponent
Holger Stünitz
University of Tromsø

Cover image and illustrations by Cindy Lizeth Urueña Suárez

Lithosphere and Biosphere Science
Department of Geology
Faculty of Science

ISBN 978-91-87847-72-1 (print)

ISBN 978-91-87847-73-8 (pdf)

ISSN 1651-6648

Printed in Sweden by Media-Tryck, Lund University, Lund 2023

Organization	Document name
LUND UNIVERSITY Department of Geology Sölvegatan 12 SE-223 62 Lund Sweden	DOCTORAL DISSERTATION
	Date of issue May 17, 2023
Author(s) Cindy Lizeth Urueña Suárez	Sponsoring organization

Title and subtitle: Metamorphism in the roots of mountain belts and its effect on rock technical properties: A case study of the Eastern Segment, Sveconorwegian orogen

Abstract

Deciphering the metamorphic evolution of the roots of mountain belts is essential for understanding deep tectonic processes involved in mountain building. The Sveconorwegian orogen in southwestern Scandinavia, formed during the Rodinia assembly in the transition between the Mesoproterozoic and Neoproterozoic Eras, has been exhumed and provides access to interior deep structural levels of the ancient mountain belt. The Eastern Segment of the Sveconorwegian Province corresponds to the underthrusting continental crustal block that was metamorphosed under variable temperature conditions and differences in the availability of hydrous fluids. As a result, the bedrock across the Eastern Segment has different mineral assemblages and textural characteristics.

This thesis investigates the metamorphic behaviour of the deep-seated bedrock in the Eastern Segment from two approaches. Bedrock is a widely exploited raw material in Sweden for use in crushed aggregate production. The performance of aggregates is steered by the textural and mineralogical properties, which, in turn, are determined by the geological processes. The first part of the study aims to assess the influence of metamorphic conditions on the technical properties of crushed bedrock aggregates. The second part focuses on the metamorphic evolution resulting from the limited introduction of hydrous fluids in a ~25 km wide discrete deformation zone with steeply dipping and anastomosing structures in the easternmost part of the Eastern Segment. At the present erosion level, this deformation zone delimits the Sveconorwegian ductile deformation to the east.

The results of the first two studies indicate that technical properties of bedrock vary systematically with the macro-fabric and microtextures across the Eastern Segment. Rocks of granitic and gabbroic compositions show a close relationship between the mode of recrystallization and the resistance to fragmentation and wear. Changes in the state of recrystallization reflect the differences in the metamorphic temperature and availability of hydrous fluids. As a result, rocks show variations in the mineral assemblage, size, and shape of the crystals. High performance of aggregates is linked to high textural complexity, which is characterized by non-uniform grain-size distributions and irregular grain boundaries. In granitic and gabbroic rocks, these textural parameters stemmed from metamorphism under low availability of hydrous fluids and at variable temperatures, below 600 °C and above 750 °C. In granites, the recrystallization of quartz and feldspar at these conditions yielded complex rock textures. In gabbroic rocks, however, the textural complexity is determined by the preservation of relict igneous textures due to limited hydration. High-grade metamorphism associated with hydration and partial melting yielded low resistance of granitic and gabbroic aggregates to fragmentation and wear. This investigation illustrates how knowledge of metamorphic processes effectively supports the prediction of functional properties of bedrock aggregates.

Two following studies focus on the metamorphic evolution within the easternmost deformation zone of the Sveconorwegian Province. Textural analysis linked to petrological and geochronological data was performed on samples from a key locality of Mesoproterozoic syenodiorite, in which the syenodioritic rock preserves different states of deformation and metamorphic recrystallization. The textural relationships show partial to complete replacements of the primary igneous minerals, including the formation of metamorphic zircon at the expense of igneous baddeleyite and zirconolite. The findings demonstrate that metamorphic reactions were induced by the influx of hydrous fluid in deformed zones. The deformation assisted the infiltration of hydrous fluid, resulting in different states of recrystallization and deformation: while fully recrystallized rocks record equilibrium at 540–600 °C and 9–12 kbar, rocks in undeformed domains remained in a metastable near-pristine igneous state. This study contributes to the understanding of the metamorphic processes that operated at depths of 35–40 km within a ductile deformation zone in the easternmost part of the Eastern Segment and the frontal parts of the Sveconorwegian orogen.

Key words Sveconorwegian, metamorphism, hydrous fluids, microtextures, recrystallization, aggregate properties.

Classification system and/or index terms (if any)

Supplementary bibliographical information	Language English
ISSN and key title: 1651-6648 LITHOLUND THESES	ISBN 978-91-87847-72-1

Recipient's notes	Number of pages 174	Price
	Security classification	

Signature: Date: 2023-03-28

Contents

List of papers

This thesis is based on the four papers listed below, which have been appended to the thesis. Paper I is reprinted under permission of Elsevier for non-commercial purposes in agreement to the editorial polices.

Paper I

Urueña, C., Andersson, J., Möller, C., Lundgren, L., Göransson, M., Lindqvist, J.-E., & Åkeson, U. (2021). Variation in technical properties of granitic rocks with metamorphic conditions. Engineering Geology, 293, 106283. https://doi.org/10.1016/J.ENGGEO.2021.106283

Paper II

Urueña, C., Möller, C., Andersson, J., Lindqvist, J. E., & Göransson, M. (2022). The effect of metamorphism on the aggregate properties of gabbroic rocks. Bulletin of Engineering Geology and the Environment 2022 81:5, 81(5), 1–27. https://doi.org/10.1007/S10064-022-02718-8

Paper III

Urueña, C. & Möller, C. Fluid-induced metamorphism and deformation at the eastern boundary of the Sveconorwegian Province. Manuscript.

Paper IV

Urueña, C., Möller, C., Plan, A. Metamorphic titanite – zircon pseudomorphs after igneous zirconolite. Manuscript.

Acknowledgements

I want to express my deepest gratitude to all the people who have been part of my doctoral process and have contributed in many different ways. First and foremost, I would like to thank my supervisor Charlotte Möller (Lotta) and my co-supervisors Jenny, Andersson, Jan-Erik Lindqvist, Mattias Göransson and Urban Åkeson. Many thanks for the enjoyable fieldwork and constructive discussions; the content of this dissertation is the product of this collaborative and fruitful work.

A special thanks to Lotta, who supported and guided me through the research, shedding light on the path with her expertise, and who also provided the *Svensk sammanfattning*. I am very grateful to Jenny, who supported me and always encouraged me with her enthusiastic mood when I was struggling with many things. Lotta and Jenny worked patiently, thoroughly, and timely on the manuscripts and always helped me deal with revisions over and over again. I thank Jan-Erik and Mattias for introducing me to the lab work on the technical properties of rocks and actively discussing concepts and interpretations.

I would like to thank the Swedish Geological Survey (*Sveriges geologiska undersökning*, SGU) and the Royal Physiographic Society of Lund for their financial support for the project and studies. I would also like to thank the rock material companies in southern Sweden that made it possible for us to visit the quarries and take samples for this project. I thank Paula, Oscar and Steffan from SGU, who kept their interest in the project and helped me with the lab work. I am grateful to NordSIM-Vegacenter for providing facilities for geochronological analysis; I thank Kestin Lindén, Martin Whitehouse and Heejin Jeon for their assistance and experimental support in working with my tiny crystals. I am very grateful to the staff of the Department of Geology at Lund University for the receptive atmosphere. The administrative staff were always available to solve technical and economic affairs, thanks to Gert, Britta, Anna, Ylva and Irma. Many thanks to Ulf Söderlund, Leif Johansson, Helena Filipsson, and Daniel Conley for their valuable academic advice during my studies.

It was a four-year journey (with half in corona times), but completing my dissertation required more than academic support, and Lotta, together with Leif, offered me their friendly company, weekend trips, nice conversations, yummy dinners and *fikas*, and showed me awesome places in southern Sweden with the charm of Swedish culture after moving so far from home. I could not forget the fantastic holidays looking at rocks, hiking mountains, and visiting fjords in Norway. Thank you so much for such amusing experiences!.

I am very grateful for the many memorable moments, *fikas*, lunches, dinners, barbecues, celebrations, game nights and evenings in and out with my PhD colleagues and PostDocs that kept the good vibes going. I met so many people from different countries, and they have left me with fond impressions. Many thanks to my office mates Ingrid, Josefin, Karolina, Miguel and Maria for the great company for a long and short time. Thanks to Constance, Qin, Julia, Paulina, Ingrid, and Chiara for the well-needed cheering words over the last month. I would also like to thank Robert and Ulla for opening their charming home to me when I first arrived in the city and generously inviting me to my first *Midsommar* celebration.

Finally, I have to thank many people for listening to me and motivating me to keep going during these four years; friends and family cheered me up from afar. A big thank you to my esteemed former mentors, Carlos Zuluaga and Matthias Bernet, for their enormous trust in me and trust that I would find the path. I also would like to thank my friends outside academia, my dearest Claudia, Isabel, Marcela, Yolanda, and many others, for their encouraging words from the other side of the Atlantic and even for being there to meet us when I came back to Bogotá. Most importantly, none of this could have been possible without my family. Thanks for making a book full of lovely messages and memories. I would like to give my warmest thanks to my parents and siblings for their valuable dedication and support throughout the years, for believing in my dreams, for helping me pursue them and for being my role model of courage. This dissertation stands as a testament to your unconditional love and encouragement.

Lo más importante, nada de esto hubiera sido posible sin mi familia. Gracias por hacer un libro lleno de lindos mensajes y recuerdos que me acompañaron cuando necesitaba fortaleza. Mi más cálido agradecimiento a mi mami, mi papi, Karen y David por su invaluable dedicación y apoyo a lo largo de los años, por creer en mis sueños e ilusiones, impulsarme a perseguirlos y a ser valiente con su ejemplo. Esta disertación es una evidencia de su amor y esfuerzo incondicionales.

Dreams are maps. Without them, we go nowhere –
Cosmos

Introduction

Mountain belts are formed by large-scale convergent movements of continental and oceanic tectonic plates that lead to convergent margins and ultimately continent-continent collision zones. As a result, the crust undergoes deformation, metamorphism, and partial melting during the mountain building. These processes yield extensive changes in the mineralogy, texture, and structure of the crust. Once the tectonic interactions dwindle, exhumation and erosion of the mountain range may lead to the exposure of deep orogenic roots. Such deeply eroded orogens allow the study of the reworking of crust and the geological processes operating at depth.

When two continents collide, one plate overrides the other (Figure 1). Continental collision has operated since at least the Paleoproterozoic (e.g., the Trans-Hudson orogen, Hoffman 1988). In places, the Proterozoic orogens expose high-temperature and high-pressure metamorphic terranes that are the exhumed deep roots of the mountain belts (Weller et al. 2021).

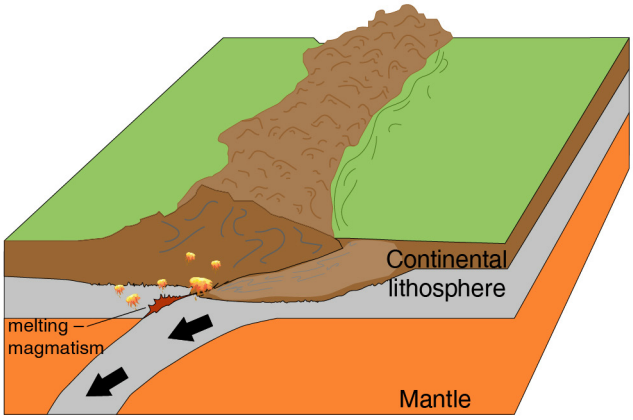

Figure 1. Schematic conceptual model for mountain belts in a continent–continent collisional setting, showing underthrusting of continental crust (lighter brown).

This thesis focuses on the metamorphic bedrock of a Late Meso- to Early Neoproterozoic collisional orogen in southwestern Scandinavia, the 1.07–0.90 Ga Sveconorwegian orogen (Bingen et al. 2021). This orogen formed during the amalgamation of the supercontinent Rodinia (Li et al. 2008) and exposes sections of formerly deeply buried continental crust (Möller et al. 2015; Möller and Andersson 2018). During the Sveconorwegian orogeny, the eastern part of the orogen, known as the Eastern Segment, experienced tectonic burial to depths of ~40 km (op. cit.). The tectonometamorphic record in the Eastern Segment is related to westward underthrusting (cf. Fig. 1) of this crustal portion beneath the western part of the orogen.

The Eastern Segment underwent deformation and metamorphism at successively higher metamorphic temperatures from east to west, grading from *c.* 550 to 800 °C and accompanied by partial melting in the high-grade metamorphic sections (Möller and Andersson 2018). Subsequent exhumation and erosion have exposed a transition within the basement (present-day erosion level), from the foreland across the bounding deformation zone and into the orogenic interior, within a formerly deep structural level. The metamorphic conditions range from epidote- amphibolite-facies in the east to high-pressure granulite-facies in the west. The metamorphic zoning across the Eastern Segment provides a unique natural laboratory for studies of the metamorphic and tectonic processes of the orogen.

The variation in the character of the metamorphic recrystallization in the Eastern Segment is also closely linked to the presence of hydrous fluids and deformation. Taken together, the variation in the metamorphic conditions (i.e., pressure, temperature, deformation, and availability of fluids) yielded considerable differences in texture, microstructures, and mineralogy of the bedrock. These petrographic characteristics also steer the technical properties of the rock. Understanding of mountain-building processes and metamorphic recrystallization is, therefore, a powerful tool for predicting the technical properties of rocks. This knowledge is of fundamental interest for construction and tunnelling in bedrock as well as for prospecting high-quality crushed bedrock aggregates.

An interdisciplinary approach

The exploitation of bedrock as a natural resource has become increasingly important as the demand for construction materials has grown. The increasing demand contrasts with the need for environmental protection, drinking water, energy saving, and reduction of CO_2 emission. High technical quality of extracted rock materials can minimize these environmental impacts. Extraction of the most suitable rocks in optimal locations (i.e., close to where they will be used; SGU, 2015) will reduce the use of chemicals and water in the production process, minimize the amount of rock waste, increase the quality of the final product (e.g., for buildings and infrastructure), and reduce transport. These improvements require the integration of process-related geology and a thorough understanding of the geological processes that steer the functionality of the rock materials. Therefore, understanding orogen dynamics is a valuable field of research for applied bedrock geology.

In Sweden, metamorphic rocks are an important source of raw materials for the production of aggregates used in the construction of infrastructure (Göransson 2018). High-quality aggregates are preferably produced from granitic rocks due to their high resistance to mechanical abrasion (Afolagboye et al. 2016; Sajid et al. 2016; Trotta et al. 2021). Although the technical properties of rocks depend on petrographic characteristics, such as mineralogy, texture, and structure (Åkesson et al. 2001; Lindqvist et al. 2007), research on crushed bedrock aggregates includes little or no information about geological processes (e.g., metamorphism and deformation) that steer such petrographic parameters. However, linking the effects of metamorphism on technical properties has a significant potential for the prediction of the functionality of aggregates (Figure 2).

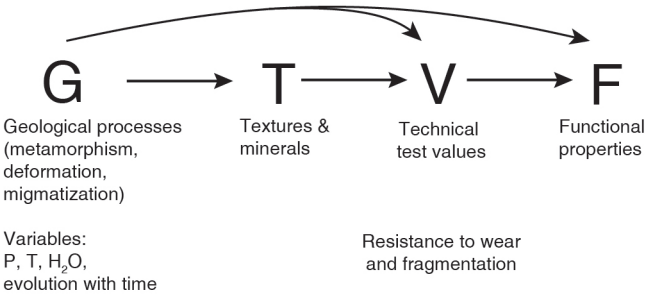

Figure 2. Flowchart illustrating the sequence of effects from geological processes (G) to the functionality of aggregates (F).

Scope of the thesis

This thesis address two primary fields of interest:

1. Variations in the technical properties of bedrock aggregates with the metamorphic conditions.
2. Progressive changes in the metamorphic recrystallization and deformation within the easternmost part of the present-day orogenic front in the Eastern Segment.

The metamorphic field gradient across the Eastern Segment of the Sveconorwegian Province enabled a systematic investigation of how the metamorphic conditions can affect the aggregate technical properties. In the first part, the study focused on metaintrusive rocks of granitic and gabbroic compositions. Granitic and gabbroic rocks have significant differences in mineralogy and texture. Consequently, they respond differently to metamorphism and deformation. Paper I documents the geological parameters that steer the technical properties of granitic aggregates, whilst paper II focuses on gabbroic rock aggregates. The results from these two publications can be used for prospecting after high-performance aggregates and are applicable to granitic and gabbroic metamorphic rocks in other geological settings.

The second part of the thesis focuses on microtextural and mineralogical relationships associated with the transformation from well-preserved syenodiorite to protomylonite. The studied rocks underwent non-penetrative deformation at epidote-amphibolite facies and recorded different states of metamorphic recrystallization. The results of petrological analysis and geochronology are presented in two manuscripts. Paper III provides an example of the style of metamorphism and deformation within the easternmost deformation zone in the basement of the Sveconorwegian orogen. Paper IV reports on metamorphic titanite + zircon intergrowths that represent pseudomorphs after igneous zirconolite. Collectively, the findings in these two manuscripts illustrate the role of hydrous fluids and deformation during the metamorphic evolution.

Background

Petrographic parameters: Fabric, texture, and microstructures

The term fabric describes the spatial and geometric arrangement of components and minerals that make up a rock (Passchier and Trouw 2005; Higgins 2006). In metamorphic rocks, however, the definitions of texture and microstructure partly overlap since texture may involve microstructural features. Commonly, texture refers to the distribution and relationships of minerals and to geometric aspects such as grain size and shape. The microstructures describe grain-scale features such as grain boundaries, mineral arrangement, and internal orientation of the crystallographic lattices of the minerals (Passchier and Trouw 2005; Song and Cao 2021).

The petrographic parameters of rocks (including mineralogy, texture, and structure) are the products of geological conditions and tectonic history. Depending on changes in physical and chemical conditions during the mountain building, the bedrock records different textures and microstructures. In the geomaterials engineering field, it is well established that the intrinsic petrographic parameters largely influence the mechanical behaviour and technical properties of rocks (Ersoy and Waller 1995; Lindqvist et al. 2007). Hence, the characterization and

measurement of these parameters allow the assessment of aggregate performance. To estimate the influence of the metamorphic conditions on the technical properties of bedrock, the quantitative and semi-quantitative parameters examined in this thesis included mineralogy, grain size distribution, grain boundary morphology, and microcracks.

Relationships between petrographic parameters and technical properties

The effects on the technical properties caused by textural and mineralogical modifications during metamorphic recrystallization, partial melting, and deformation are summarized below.

Mineralogy

The influence of mineralogy on the resistance to fragmentation and wear has been partly associated with the physical properties of the mineral (e.g., crystal shape and hardness). For instance, mineral hardness may enhance rock strength. Quartz and feldspars are generally harder than other silicates and ferromagnesian minerals. Therefore, high quartz and feldspar contents increase the resistance of rocks to mechanical abrasion (Tuğrul and Zarif 1999; Miskovsky et al. 2004). In contrast, micaceous minerals are mechanically fragile due to their flakiness. Thus, high content of thin and elongated minerals is linked with a reduction in the resistance to mechanical abrasion (Brattli 1992; Miskovsky et al. 2004).

Rock fabric

Anisotropic rock fabrics are characterized by oriented planar and linear structures. Foliations, lineations, and veins represent micro- to meso-scale heterogeneities that commonly affect the aggregate technical properties. If the foliation is defined by micas or other flaky minerals, the individual foliation planes constitute large discontinuities. The negative effect of mica on the resistance to fragmentation is more commonly the result of the orientation and distribution of mica crystals than the amount of mica (Åkesson et al. 2003; Göransson et al. 2004). Indeed, randomly oriented micas can increase rock strength since they may act as energy barriers for propagating cracks (Miskovsky et al. 2004). The anisotropy of the rock fabric can be quantitatively described by the foliation index (FIX; Åkesson et al. 2003).

Grain size and grain morphology

The grain size and grain size distribution also have a significant influence on the resistance to fragmentation and wear. Unevenly distributed fine-grained size fractions usually boost the quality of the aggregates (Lundqvist and Göransson 2001). In contrast, coarse grain size minerals forming a granoblastic texture typically decreases the rock strength.

The nature and shape of grain boundaries also have an important role. High irregularity of grain shapes and interlocking of grains increase the resistance to fragmentation (Åkesson et al. 2003). A qualitative assessment of grain boundary shape in rocks with even and uneven grain size distributions may be completed using the scheme proposed by Hellman et al (2011; Figure 3). Nonetheless, areal and grain perimeter measurements provide an approach to grain shape quantification.

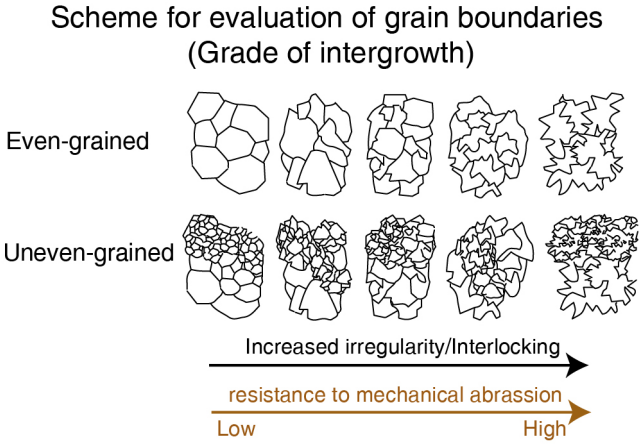

Figure 3. Scheme for qualitative evaluation of the grade of intergrowth and irregularity of grain boundaries in rock with even and uneven grain size (adapted from Hellman et al. 2011). Arrows indicate the increasing resistance to mechanical abrasion with higher irregularity of grain boundaries.

Microcracks

Open slots, such as microcracks developed during brittle deformation, may act as pathways for water or water reservoirs; eventually, the water flow cause dissolution or frost damage (Hellman et al. 2011). A high frequency of microcracks commonly decreases the resistance to fragmentation. However, discontinuities in the rock fabric may hinder microcrack propagation. Such discontinuities include irregular grain boundaries, poly-mineral grain contacts, and porosity. Once the crack reaches a discontinuity, the stress is dissipated. Nevertheless, cracks can easily propagate across mono-mineral contacts.

Microstructures and microtextures – changes with metamorphic conditions

This section provides a description of microstructures and microtextures that are related to the metamorphic processes in the Eastern Segment.

Deformation-induced microstructures at subsolidus conditions

Regional metamorphism is normally accompanied by deformation. The type of deformation depends on several factors, such as rheology, temperature, pressure, strain rate, and the presence of hydrous fluid. Brittle deformation dominates in the uppermost crust, whereas ductile deformation operates at high lithostatic pressure (i.e., depth) and, particularly, at high temperature (Gomez-Rivas et al. 2020).

Many deformation mechanisms can be identified by grain-scale microstructures, which reflect different temperature and strain conditions. Low-temperature mechanisms under brittle conditions include intragranular fracturing, frictional sliding, and grain rotation (Figure 4a–b). As temperature increases, deformation is accommodated by ductile deformation mechanisms, which include intracrystalline deformation, recovery, recrystallization, and diffusion creep (Vernon 2004; Passchier and Trouw, 2005).

Crystal plasticity refers to the migration of the lattice defects within the crystals and occurs predominantly at the brittle-ductile transition. During intracrystalline deformation, the dislocations glide along specific crystallographic planes, known as a slip system (Passchier and Trouw 2005; Gomez-Rivas et al. 2020; Figure 4c–e). An effect of slipping is the development of a preferred lattice and shape orientation. Other microstructures that reflect intracrystalline deformation include undulous extinction, kinking (e.g., in micas), deformation lamellae (e.g., in quartz), and mechanical twinning (e.g., in calcite and feldspars; Vernon 2004; Passchier and Trouw 2005).

The accumulation of lattice defects leads to an increase in the internal strain energy of the crystal (Passchier and Trouw 2005; Gomez-Rivas et al. 2020). A high-strain accumulation yields ribbons of elongated crystals. However, as ductile deformation progresses, the strain energy is reduced by recovery and recrystallization (i.e., dynamic or static, the latter after the strain rate decreases). Furthermore, the presence of fluid along grain boundaries enhances the recovery and recrystallization processes (Passchier and Trouw 2005).

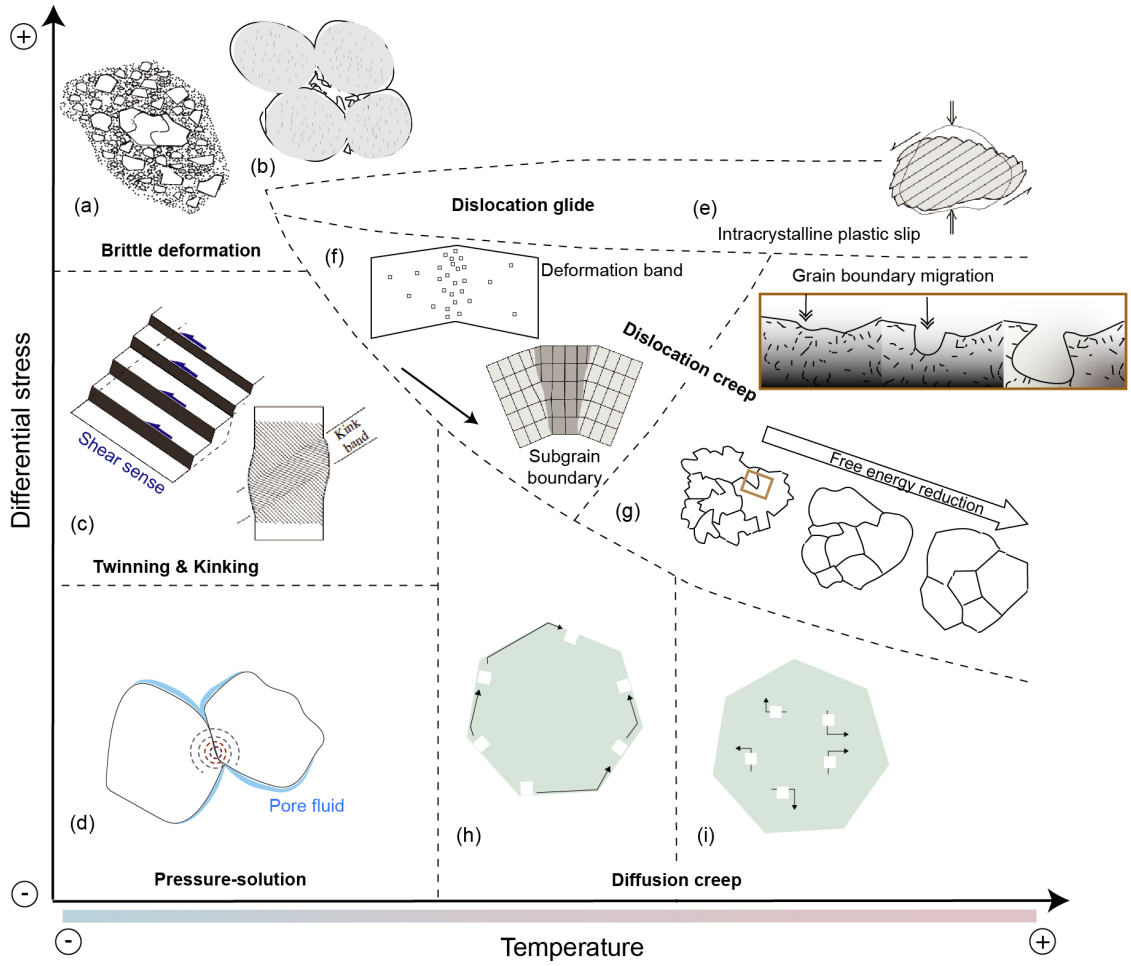

Figure 4. Summary of common deformation mechanisms, showing the variations with temperature and differential stress (**Bold**: mechanism map adopted from Gomez-Rivas et al. 2020). (a) Cataclasis. (b) Frictional grain boundary sliding producing spalling or flaking. (c) Mechanical twinning and Kink band formation (d) Pressure solution at grain contacts involving dissolution and reprecipitation. (e) Intracrystalline deformation, involving dislocation glide. (f) Recovery. Concentration of dislocations in deformation bands and subsequent formation of subgrain boundaries. (g) Evolution of the recrystallization mode from grain boundary migration to grain boundary area reduction.(h) Cobble creep, vacancies migrating along grain boundaries. (i) Nabarro-Herring creep, vacancies migrating through the crystal lattice.

During recovery, the lattice defects merge into deformation bands that eventually transform to distinct subgrain boundaries (Figure 4f; Passchier and Trouw 2005). Continued accumulation of dislocations along a subgrain boundary results in the formation of a grain boundary, dividing the former crystal into separate crystals.

Dynamic recrystallization processes involve modifications of both the shape and size of crystals. At low temperatures, recrystallization involves the neoformation of very fine-sized crystals (neoblasts) by the *bulging* mechanism (cf. Passchier and Trouw 2005). Increasing temperature causes the grain boundaries to become increasingly mobile, leading to grain boundary migration (Figure 4g; Gomez-Rivas et al. 2020). Thus, this dynamic recrystallization yields highly irregular crystals with sutured grain boundaries. However, the neoblasts formed along the grain boundaries are unstrained, and their size partly depends on the differential stress (Best 2003; Fossen 2010).

Recrystallization evolves to minimize total free energy in the system. High-energy crystals are replaced by lower-energy ones. If the temperature is high enough, eventually, the grains are fewer, coarser with more regular shapes and typically form a polygonal arrangement (Fossen, 2010). Less complex grain morphologies with lobate to straight boundaries are diagnostic of recrystallization under strain-free (or static) conditions (Passchier and Trouw 2005). At this stage, vacancies in the crystal are accommodated by diffusion creep (Figure 4h–i; Gomez-Rivas et al. 2020).

Reaction textures at subsolidus conditions

This section contains a brief description of two types of microtextures developed as a consequence of changes in the physical conditions (pressure and/or temperature): exsolution and replacement textures. These textures provide evidence of mineral reactions.

Exsolution texture is identified as intergrowths or lamellae of minerals that belong to a solid solution series (e.g., albite and K-feldspar). The immiscibility of two or more phases of the solid solution is caused by variations in the physical conditions(Song and Cao 2021). Generally, exsolutions are produced due to cooling or decompression (op. cit.).

Replacement textures are the result of mineral reactions during the metamorphic evolution (Song and Cao, 2021). The mineral replacements can be partial (reaction rims or coronas) or complete (pseudomorphs). Partial replacements indicate that the metamorphic reaction was not completed.

The coronitic texture consists of a relict mineral rimmed by a monomineralic or polymineralic corona (Song and Cao 2021). The phases in the corona represent the products of the reaction sequence. In some cases, the new minerals form vermicular intergrowths (symplectite). Pseudomorphs are the product of a complete mineral replacement. In a pseudomorph, the shape of the former mineral is still recognizable, but it has been replaced by another mineral or intergrowths of other minerals(Putnis and John 2010). The new mineral(s) is(are) a product of the metamorphic reaction and commonly preserves the major elements of the precursor phase. Some pseudomorphs provide insight into the fluid-rock interaction process, in which the dissolution and precipitation mechanisms are closely coupled(op. cit.).

Partial melting-related structures and textures

Partial melting of rocks takes place at high-temperature conditions. In addition to temperature and pressure, the availability of hydrous fluids is a critical factor in producing high volumes of melt in different crustal settings (Stuart et al. 2017). Melting can take place in either water-saturated or water-undersaturated environments. Melting can occur at relatively low temperatures (above 630 ºC) if water is present as a free fluid. In contrast, fluid-absent melting that takes place at temperatures from ~700 °C by dehydration of hydrous minerals, such as muscovite, biotite, and amphibole (Sawyer et al. 2011; Weinberg and Hasalová 2015; Stuart et al. 2017; Schwindinger et al. 2019). When the mineral reactions produce a new solid phase in addition to the melt, it is known as incongruent melting.

Regardless of the water-saturation conditions, partial melting results in the formation of a migmatite. Migmatitic rocks consist of leucosome (the partial melt) and mesosome (the modified remnant); some migmatites include a melanosome, which is made up of minerals formed by different processes (e.g., Schmid et al. 2004; Sawyer 2008). It is noteworthy that the formation of peritectic minerals in migmatites is indicative of incongruent melting reactions, at suprasolidus P–T conditions (Weinberg and Hasalová 2015).

The composition and structure of a migmatite depend mainly on bulk composition, amount of melting, and strain. Deformation is partitioned into the weakest parts (i.e., the melt) and can produce complex geometries (Sawyer and Brown 2008). Migmatite classification is based on the melt fraction, and their structures vary according to syn-anatectic strain (Sawyer 2008). At higher differential stress, the melt is concentrated in layers parallel to the rock foliation (Sawyer 1999).

As a rule, hydrous fluid promotes recrystallization, metamorphic reactions, crystal growth, and smoothening of grain boundaries. The molten rock portions develop isotropic and equilibrated fabrics with even-grained polygonal textures (Passchier and Trouw 2005; Holness 2008). Some typical microstructures produced during partial melting include simple twinning of K-feldspar, cuspate grain boundaries, oscillatory zoning, and mi-

crogranophyric intergrowths (i.e., quartz and alkali feldspar), which may resemble igneous mineral microstructures (Vernon 2011). However, these textural features are not always preserved after cooling.

Geological and tectonic context

This chapter briefly summarizes the geological evolution during Sveconorwegian mountain building in the eastern part of the Sveconorwegian Province. The tectonic and petrological records bear witness to deep-seated rocks formed during collisional orogeny.

Sveconorwegian Province

The Sveconorwegian orogen is a Late-Mesoproterozoic orogenic belt commonly interpreted to have formed by continental collision during the Rodinia assembly (Bingen et al. 2008, 2021; Möller et al. 2015). However, other interpretations propose that the Sveconorwegian Province represents an accretionary margin (Slagstad et al. 2013, 2020; Coint et al. 2015) unrelated to the assembly of Rodinia (Kulakov et al. 2022; Slagstad et al. 2023). Based on available petrological and geochronological data, Bingen et al. (2021) propose that the Sveconorwegian orogen is a product of a large, hot, and long-duration continent-continent collision between proto-Baltica and another plate in the Rodinia-forming context.

The Sveconorwegian Province is a >500 km wide belt of regional deformation and metamorphism extending across southern Scandinavia. It is made up of two main lithotectonic megablocks (Figure 5): the Sveconorwegia in the west, which include four segments (Telemarkia, Kongsberg Bamble, and Idefjorden) composed of dominantly Mesoproterozoic igneous protoliths, and the Eastern Segment whose protoliths formed as a part of a large granitic belt in the Paleoproterozoic active margin of Fennoscandia, following the Svecokarelian accretionary orogeny (Stephens and Wahlgren 2020b; Bingen et al. 2021). The two lithotectonic blocks are separated by the Mylonite Zone, a conspicuous west-dipping Sveconorwegian ductile shear zone (Stephens et al. 1996; Andersson et al. 2002; Viola and Henderson 2010; Viola et al. 2011). The exhumation of an eclogite-bearing nappe in the Eastern Segment footwall, directly underlying Sveconorwegia, is one reason suggesting that the Mylonite Zone represents a major Sveconorwegian lithotectonic boundary (Möller et al. 2015). This was initially proposed by Andersson et al. (2002), Austin-Hegart et al. (2007), and Petersson et al. (2015a).

The Sveconorwegian Province records a metamorphic evolution from 1.07 to 0.90 Ga. An earlier metamorphic event between 1150 and 1120 Ma is recorded in Kongsberg and Bamble, characterized by amphibolite- to granulite-facies metamorphism (Engvik et al. 2016). The Kongsberg–Bamble lithotectonic units also record bi-modal magmatism between 1280 and 1145 Ma (Bingen et al. 2021). A subsequent quiet period was followed by the main Sveconorwegian tectonometamorphic phase in Sveconorwegia from 1065 to 1000 Ma (Bingen et al. 2021). During this phase, Telemarkia and Idefjorden underwent metamorphism at variable conditions, including partial melting and magmatism (op. cit). High-pressure granulite-facies metamorphism in the eastern part of Idefjorden around 1050 Ma contrasts with lower-pressure granulite-facies metamorphism in Telemarkia that culminate at UHT conditions (1030–1005 Ma; Bingen et al. 2021).

The late Sveconorwegian stage (960–960 Ma) is characterized by the Eastern Segment underthrusting the western Sveconorwegia (Bingen et al. 2008, 2021; Tual et al. 2017; Möller and Andersson 2018). The metamorphic evolution during this collisional stage is reflected in a metamorphic field gradient across the Eastern Segment, which exposes a transition from greenschist to upper-amphibolite and granulite facies associated with partial melting (Möller and Andersson 2018). At the contact with Idefjorden, a section of the underthrusting Eastern Segment was metamorphosed at eclogite facies conditions and thereafter exhumed to *c*. 40 km depth (Möller et al. 2015; Tual et al. 2017; Möller and Andersson 2018). The eastward exhumation of the eclogite-bearing unit was associated with the metamorphism of the internal section of the Eastern Segment at *c*. 800 °C and 10 kbar (Möller et al. 2015; Tual et al. 2017).

The collision was followed by regional extension and 980–940 ma dolerite intrusions in the eastern part of the orogen and east thereof (Söderlund et al. 2005; Gong et al. 2018). After 930 Ma, the late- to post-Sveconorwegian collapse involved granitic magmatism in the western Sveconorwegian terranes, extension, and exhumation (Andréasson and Dallmeyer 1995; Söderlund et al. 1999; Bingen et al. 2008, 2021; Ulmius et al. 2018; Ripa and Stephens 2020; Stephens and Wahlgren 2020b). At the present-day erosion level, Mesoproterozoic sedimentary rocks in the foreland of the Eastern Segment are regarded as a remnant of the sedimentary cover upon the Paleoproterozoic basement (Almesåkra Group sediments; Rodhe, 1992; Figure 5).

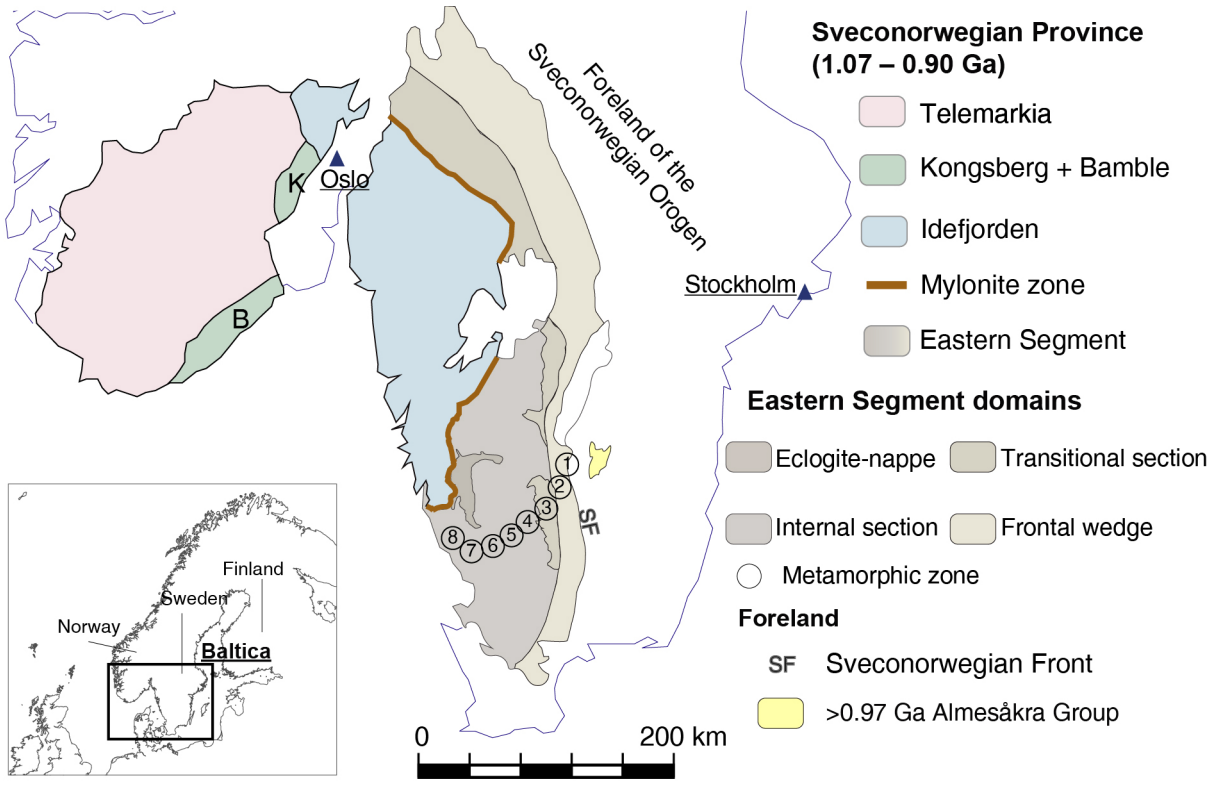

Figure 5. Sketch lithotectonic map of the Sveconorwegian Province in southwestern Scandinavia, showing the nomenclature of lithotectonic units and subdivision of the Eastern Segment (after Möller et al, 2015) The metamorphic zones proposed by Möller and Andersson (2018) are indicted by the number (a detailed map is presented in papers I and II).

Metamorphism in the Eastern Segment

The Eastern Segment is the reworked margin of the Paleoproterozoic Fennoscandian continent. Bedrock in the Eastern Segment is part of a coherent Paleoproterozoic magmatic belt known as the Transscandinavian Igneous Belt (Söderlund et al. 2002; Möller et al. 2007; Petersson et al. 2015b; Möller and Andersson 2018). These rocks are mainly granitic, granodioritic to quartz–monzonitic and quartz–monzodioritic in composition, with subordinate metagabbro and metadolerite (Stephens and Wahlgren 2020b). The protolith ages of the dominant granitic intrusives range from 1.73 to 1.66 Ga (Petersson et al. 2015b; Stephens and Wahlgren 2020b). Volumetrically smaller intrusions of granite–syenite intruded at 1.47–1.38 Ga and 1.22–1.18 Ga (Hubbard 1989; Andersson et al. 1999; Christoffel et al. 1999; Jarl 2002; Söderlund and Ask 2006; Petersson et al. 2015b; Ulmius et al. 2015; Johansson 2021). Mesoproterozoic mafic magmatism is recorded at 1.57 Ga (Söderlund et al. 2004, 2005; Söderlund and Ask 2006; Beckman et al. 2017), 1.47-1.44 Ga (Brander and Söderlund 2009), 1.42-1.39 Ga (Hansen et al. 2015), 1.27-1.25 Ga (Brander et al. 2011), and 1.22-1.20 Ga (Larsson and Söderlund 2005; Söderlund et al. 2005; Söderlund and Ask 2006). Mafic magmatism in the 1.47-1.20 Ga interval also included the emplacement of massif anorthosite (Söderlund and Ask 2006; Brander and Söderlund 2009).

Whereas the ~1.2 Ga syenite, gabbro, and anorthosite intrusions has been interpreted as a product of bimodal magmatism during a regional E–W extension, the magmatism at 1.47–1.38 Ga has been associated with the Andean-type Hallandian orogeny (Hubbard 1975; Söderlund et al. 2002; Möller et al. 2007; Ulmius et al. 2015; Stephens and Wahlgren 2020a). The Hallandian tectonometamorphic event involved low-pressure granulite-facies metamorphism and partial melting at 1.45 Ga (Ulmius et al. 2015). However, in most parts of the Eastern Segment, the Sveconorwegian metamorphism has overprinted the Hallandian metamorphic record (op. cit.).

The Sveconorwegian ductile deformation in the Eastern Segment included several phases of folding (Möller et al. 2015; Piñán-Llamas et al. 2015; Tual et al. 2015). The regional foliation is defined by a near-penetrative and, most commonly, gently to moderately dipping gneissic foliation. In the steeply dipping 25 km wide deformation zone, that bounds the Sveconorwegian Province to the east (the Frontal wedge, Figure 5), deformation wanes eastward.

Differences in metamorphic grade, style of deformation, and presence of migmatization across the Eastern Segment were used as a basis for sub-division of the segment into three sections (Möller et al. 2015; Möller and Andersson 2018). From east to west, the three sections are the Frontal wedge, the Transitional section, and the Internal section (Figure 5). In the Frontal wedge, the Sveconorwegian metamorphism grades from greenschist-fa-

cies or unmetamorphosed in the east to amphibolite-facies in the west (Möller and Andersson 2018). This section is a ~25 km wide steeply dipping, and non-penetrative deformation zone (e.g., Wik et al. 2006); in its northen part, the zone is wider and fan-shaped (Wahlgren et al. 1994). The Transitional section exposes penetratively gneissic and generally non-migmatitic rocks. Mafic rocks are garnet-rich amphibolite and subordinate coronitic metagabbro. In the Transitional section, Sveconorwegian deformation occurred under high-pressure amphibolite-facies conditions (c. 10–12 kbar; Söderlund et al. 2004). The km-scale folds plunge shallowly to the east (Möller et al. 2015).

The Internal section consists of high-grade and migmatitic orthogneisses, garnet-amphibolite, and high-pressure granulite-facies rocks. Metamorphic conditions reached high-pressure granulite- and upper amphibolite-facies. Geothermobarometry of mafic rocks has yielded temperatures between 680 and 795 °C and pressures at 8–12 kbar (Johansson et al. 1991; Wang and Lindh 1996; Möller 1998). Partial melting is common in both felsic and mafic rocks. In parts within this section, cross-cutting and undeformed pegmatites set a lower age bracket for the regional ductile deformation at ~960 Ma (Möller and Söderlund 1997; Andersson et al. 1999; Christoffel et al. 1999; Möller et al. 2007).

Furthermore, the Internal section hosts an eclogite-bearing terrane that testifies to the tectonic burial of a part of the Eastern Segment continental crust, beneath Sveconorwegia, at depths of at least 65 km (Möller et al. 2015; Tual et al. 2017). The age of eclogite metamorphism was set at 988 ± 6 Ma (Möller et al. 2015). The eclogitization was followed by tectonic exhumation, simultaneous with regional-scale high-pressure granulite- and upper-amphibolite-facies metamorphism in the Internal section (Möller and Andersson 2018).

The mineral assemblages and textures produced by metamorphism differ between the granitic and gabbroic rocks of the Eastern Segment. The gabbroic rocks show pronounced changes in the mineral assemblage, whilst, in granitic rocks, the changes are dominated by the recrystallization mode of the minerals. Based on mineral assemblages in Fe-Ti-rich metagabbro, Möller and Andersson (2018) suggested eight metamorphic zones in the Eastern Segment (Figure 5). The field and petrographic observations are summarized below.

In zones 1 and 2, undeformed rocks generally remain almost unaffected by metamorphism. The undeformed gabbroic rocks partly preserve primary igneous textures and minerals. Commonly, dark igneous minerals are surrounded by coronas of fine-grained metamorphic minerals. The weakly deformed varieties develop an anastomosing fabric defined by coarse-grained relicts of igneous plagioclase and dark minerals wrapped by a fine-grained recrystallized matrix. Deformed metagabbro contains blue-green hornblende, plagioclase, Fe–Ti oxide, and biotite, locally with titanite and epidote; in zone 2, garnet is present.

Metamorphic zone 3 corresponds to the Transitional section. Metamorphic conditions reached high-pressure amphibolite facies. Most felsic rocks have a penetrative gneissic fabric that is folded on the map scale. The orthogneisses are either non-migmatitic or underwent incipient partial melting. Gabbroic rocks vary from near-pristine to penetratively gneissic with hornblende, garnet, metamorphic plagioclase, Fe-Ti-oxide, biotite, and locally titanite. The dominant textural feature in weakly deformed metagabbros is a coronitic texture, where garnet and amphibole have preferentially grown the grain boundaries between igneous plagioclase and ferromagnesian minerals.

Zones 4 to 6 are part of the Internal section. Most granitic and mafic rocks have undergone partial melting, and leucosome is common. Leucosome developed stromatic, net, dilatation, and patch structures. Typically, the rocks are penetratively deformed and folded at the outcrop and map scale. In zone 4, non-migmatitic and less deformed metagabbro consists of olive-green hornblende, garnet, plagioclase, biotite, and Fe-Ti-oxide. In zone 5, clinopyroxene appears in metagabbro, and in zone 6, metamorphic orthopyroxene is also present.

Zones 7 and 8 are located in the westernmost part of the Internal section. In zones 7 and 8, the rocks reached high-P granulite- and upper amphibolite-facies conditions at 700–800 °C and 8–11 kbar (Johansson et al. 1991; Wang and Lindh 1996; Möller 1998). Garnet amphibolites include pockets and thin layers of leucosome that contain megablasts of peritectic orthopyroxene (up to 5 cm) and/or garnet (4–20 cm).

Methods and analytical techniques

Measurements of rock technical properties

The suitability of the bedrock for the production of crushed rock aggregates in road or railway constructions can be assessed from tests of the mechanical performance of the rocks. In this thesis, two reference methods based on mechanical abrasion of rock aggregates were used to measure their resistance to fragmentation and wear: Los

Angeles (LA; SS-EN 1097-2, 2010) and Micro-Deval (M_{DE}; SS-EN 1097-1, 2010). The technical tests followed the procedures applied at the bedrock laboratory in the Geological Survey of Sweden (Uppsala).

The functionality of rock aggregates is determined by the technical and mineralogical properties of the rocks. Mortensen and Göransson (2018) proposed a classification for road and railroad aggregates based on the correlation between Los Angeles and Micro-Deval values. This classification categorizes the aggregate performance into 4 classes according to the potential use of the aggregate (Table 1).

Table 1. Classification of road and railroad aggregates based on mechanical test values proposed by the Geological Survey of Sweden (SGU; after Mortensen and Göransson 2018). * Any material that meets both or either of the LA or M_{DE} values.

Classification	Functionality	Technical values for road construction	Technical values for railroad construction
Highest quality Class 1	Asphalt paving Suitable for ballast of superstructures and frost isolation layer	%LA < 30 %M_{DE} < 7 %micas <30	%LA ≤ 25 %M_{DE} < 17 %micas <10
Class 2	Asphalt base courses Suitable for ballast of substructures and frost isolation layer	%LA < 30 %M_{DE} 7–14	%LA 25–30 %M_{DE} < 17
Class 3*	Unbound layers Only can be used for frost isolation layer	%LA > 30 %M_{DE} > 1	%LA 30–50 %M_{DE} 17–24
Lowest quality Class 4*	Inappropriate for use in road and railroad constructions	%LA > 50 %M_{DE} > 30	%LA > 50 %M_{DE} > 24

Sample preparation

The technical tests required about 80 kg of fresh rock material per sample. The first step of crushing was done using a rotational jaw crusher (Svedala-Arbrå R 50-26-64), followed by a second step using a smaller jawbreaker (Morgårdshammar A23). Then, the crushed rock material was sieved in five different mesh sizes, i.e., >16 mm, 16–14 mm, 14–11.2 mm, 11.2–10 mm, and <10 mm.

The density (ρ) was determined by a hydrostatic weighting of 600 g of the 16–14 mm fraction. The sample was weighed at both dry and wet conditions (in water at room temperature, ρ = 0.998 g/cm^3). The density was calculated following equation (1):

$$\rho = \frac{dry\ sample\ weight \times water\ density}{(dry\ sample\ weight - wet\ sample\ weight)} \qquad (1)$$

$$\rho = \frac{600(g) \times 0.998\ (g/cm^3)}{[600 - wet\ weight](g)}$$

To perform technical tests were used 6 kg of sample from the fractions 10–11.2 mm and 11.2–14 mm.

Los Angeles Test

The resistance to fragmentation of aggregates is estimated by Los Angeles test (LA), which was carried out following the EN 1097-2 standard method (EN 1097-2, 2010). Five kilograms (5 kg) from the 10–11.2 and 11.2–14 mm fractions are rolled with 11 steel balls (Ø = 45–49 mm) in a horizontal axis rotating drum that has an internal rib. For 30 minutes, the machine runs 500 revolutions, and the sample and the steel balls are lifted by the rib to the top of the drum. When the material falls to the bottom, it is fragmented by the impact of the steel balls. Once the test is completed, the material is sieved for 5 minutes, and all fractions above 1.6 mm in size are rinsed in water and dried in an oven at 110 ± 10 ºC. The resulting dry sample (i.e., ≥ 1.6 mm fraction) is weighed to calculate the material loss.

The LA value indicates the percentage of loss of material during fragmentation and is calculated from equation (2), where m_i is the initial mass of the sample (i.e., 5000 g), and m_f is the final mass (in grams) retained in the 1.6 mm mesh. The LA value appraises how much the aggregate will resist the impact of the traffic load. Low LA values (i.e., low percentage of mass loss) correspond to high resistance to fragmentation. Conversely, high LA values (i.e., a high percentage of mass loss) imply that the material has a low resistance to fragmentation.

$$LA = \%\ of\ loss = \frac{(m_i - m_f)}{50} \qquad (2)$$

Micro-Deval Test

The Micro-Deval test method (M_{DE}) measures the resistance to wear. The test was carried out according to EN 1097-1 standard method (EN 1097-1, 2011). For the

test, 0.5 kg of the 10-14 mm sample fraction is placed in a vertical axis rotating drum with 5 kg of steel balls (Ø = 10 mm) and 2.5 l of water. After 2 hours of rotation at 120 revolutions per min, the steel balls are removed with a magnet, and the specimen is wet-sieved. The fraction retained in the 1.6 mm mesh is rinsed, dried in an oven at 110±10 ºC, and weighed. The test is performed twice to check reproducibility.

The total loss of material after the test corresponds to the M_{DE} value, which is calculated for each specimen following equation (3). The term m_i is the initial mass of the sample (i.e., 0.5 kg), and m_f is the final mass (in kg) retained at the 1.6 mm mesh. A low M_{DE} value indicates high resistance to wear, whilst a high M_{DE} value correlates with low resistance to wear and, thus, poor aggregate technical properties.

$$M_{DE} = \%\ of\ loss = \frac{(m_i - m_f)}{5} \quad (3)$$

Textural analysis

The textural analysis included a qualitative description and quantitative assessment of the petrographic parameters that define the fabric (i.e., grain shape, grain size, grain boundaries, intergrowths between phases), determination of the modal content of minerals, and microstructures. Mineral identification and documentation of microstructures were performed using optical and electronic microscopy. The observations and measurements were correlated with field relations and macro-fabric parameters such as foliation, lineation, and migmatitic structures (e.g., patch, dilatation, stromatic). The quantification of textural parameters was done from two-dimensional (2D) measurements using several techniques described below and summarized in Figure 6.

Modal point counting

The modal proportions of minerals were determined by point counting of 500 points per thin section. The analysis was done using a standard polarizing optical microscope (Olympus, BX51) with an integrated digital point counting system (PetroG). The relationships between the mineral phases, such as mineral intergrowths, reaction textures, exsolution textures (i.e., lamellae), and fabric orientation, were also documented. The modal amounts of the minerals let to correlate the proportions of quartz, feldspars, and micaceous minerals with the technical properties of the sampled rocks.

Grain morphology and grain size distribution

The geometrical parameters of crystals were estimated from the automatic processing of thin sections scanned in polarised light and using the software ImageJ (open-source; Rasband, 1997). The image processing applied filters for the transformation into binary images and contouring of the grain boundaries (Figure 6, step 2).

The complexity of the grain boundary was determined by calculating the ratio between the grain perimeter and the surface area of the grain. A high value indicates that the crystal has a complex grain boundary morphology. Data were statistically treated, and the estimations of grain boundary morphology for each sample are based on the mean value.

The maximum Feret's diameter, defined by the longest distance between two points on the grain boundary, was used to determine the grain size (Figure 6, step 2).

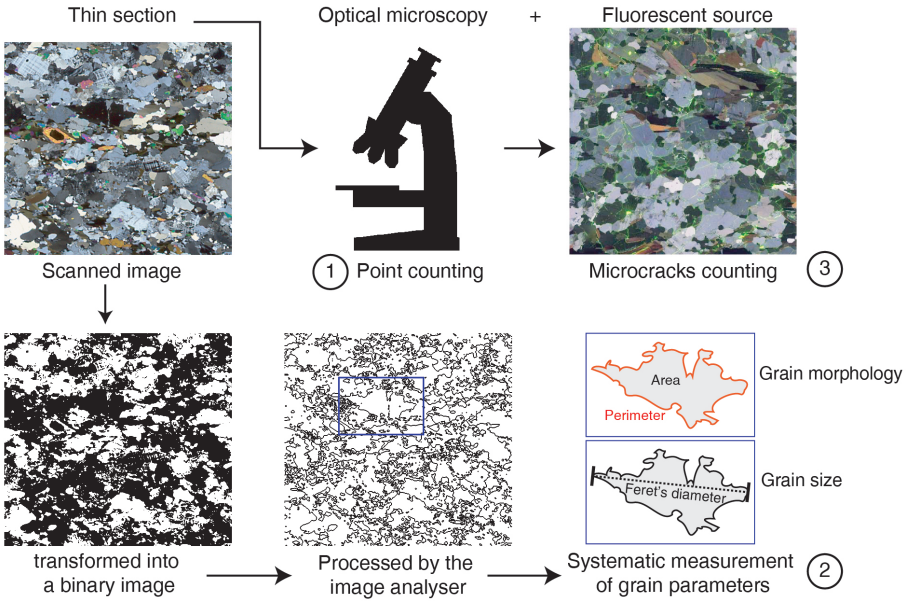

Figure 6. Simplified procedure for the analysis and measurement of petrographic parameters, following 3 stages of sequential analysis: (1) conventional petrography and modal mineral determination. (2) Automated image-based analysis to measure grain size, grain shape, and grain boundary morphology. (3) Analysis of microcraks, combining fluorescent and polarized microscopy.

The 2D grain size measurements were statistically treated to generate crystal size distribution curves. The curve shape indicates the proportions between fine and coarse crystals in the rock.

Microcracks

The analysis of microcrack frequency was used as an indirect estimate of local differences in the paleo-stress field. For this analysis, the thin sections required a mixture of epoxy with fluorescent dye. The fluorescent dye fills and highlights the microcracks. Hence, these can be recognized using an optical microscope with a fluorescent light source (Figure 6, step 3). Fluorescent and polarized microphotographs were overlapped to identify the different types of microcracks classified as intercrystalline, trans-crystalline, and grain boundary cracks. The analysis comprises counting the number of cracks intersecting traverse lines spaced at 1 mm in an area of 100 mm^2 (in two perpendicular sets of lines). The linear frequency of microcracks was calculated as the microcrack number per millimetre in the grid, which has a total length of 100 mm.

Electron microscopy

Microtextures and microstructures were imaged using a field emission scanning electron microscope (FE-SEM, Tescan Mira 3) at the Department of Geology, Lund University.

Secondary and backscattered electron imaging (SE–BSE)

Secondary and backscattered electron images are produced when an accelerated high-energy electron beam scans the specimen surface. The electrons interact with the atoms in the sample to produce reflected, bounced, diffracted, or transmitted signals. The information generated by these energy signals depends on the depth of the electron beam penetration.

At the most superficial level, the sample ionizes, yielding low-energy secondary electrons that reflect the surface topography (i.e., SE images). Electrons that reach deeper levels have multiple interactions with the atoms in the sample and produce high-energy backscattered electrons (BSE). The intensity of the backscattered signal varies as a function of the atomic number (Z) of elements. Lighter elements (i.e., small Z) yield a weaker backscattered signal than heavier elements. Therefore, the backscattered electrons indirectly reproduce compositional images based on the average atomic number. The BSE images were used to document some compositional variations in the analysed minerals.

Electron backscattered diffraction (EBSD)

Electron backscattered diffraction (EBSD) is a technique based on the capture of backscattered electron patterns, which provide crystallographic information for phase identification and microstructural characterization (Wilkinson and Britton 2012). The spectrum acquisition requires that the sample is mounted on a tilted specimen holder at a 70° angle. The diffraction pattern consists of several bright bands limited by dark lines and is known as the 'Kikuchi pattern'. The geometry of a Kikuchi pattern is interpreted as the gnomonic projection of the crystal lattice (Schwartz et al. 2009). The angles between bands correlate with the angles of crystallographic planes (Nickolsky and Yudintsev 2021).

For the analysis, the sample preparation includes a final polish with 0.25 μm colloidal silica and a *c*. 5 nm thick carbon coating of the thin section. This preparation reduces diffraction interference and charging effects during EBSD analysis. This analytical technique was used for an attempted analysis of the mineral zirconolite (paper IV). The EBSD data were collected using an Oxford Instrument AZtec system and a Nordlys detector. The Kikuchi pattern was indexed for the mineral of interest in the AZtec database, and the image was enhanced and post-processed in the module *Twist* of the *HKL Channel5* software.

Geochemistry

Whole-rock geochemistry

Bulk chemistry analysis aimed to determine the major and trace element composition of granitic and gabbroic samples in the Eastern Segment. The sample preparation included crushing, grinding, sample slit, and homogenization, followed by fine grinding to a rock powder. Part of the sample was fused in lithium metaborate/tetraborate and diluted by nitric digestion. The acid digestion process included four acids and an ultra regia acid. The major oxides and minor elements (including Si, Al, Fe^{3+}, Mg, Ca, Na, K, Ti, P, Mn and Cr) were determined by inductively coupled plasma optical emission spectroscopy (ICP-OES). Traces and rare earth elements (REEs) were measured using inductively coupled plasma mass spectrometry (ICP-MS). Total C and S were determined by infrared spectroscopy using a LECO instrument. The analytical procedures were performed by ALS Scandinavia AB in Sweden and Acme Analytical Laboratories in Canada.

Mineral chemistry

Mineral composition was used for phase identification and geothermobarometric calculations.

Energy dispersive spectrometry (EDS)

This technique is based on the measurement of the energy of X-rays. The X-rays are produced when an electron shifts energy level. This shift is induced by electrons from the high-energy source that hit the inner electron shell of atoms in the mineral, ejecting a core-shell electron. The vacancy is filled by a higher energy electron from the outer shells, releasing X-rays. The EDS detector collects and distributes the X-rays into an energy spectrum. Each energy peak in the spectra is characteristic of a specific element in the analysed mineral.

Quantitative mineral chemistry analyses were performed using an Oxford instrument energy-dispersive X-ray (EDS) system coupled to the FE-SEM, Tescan Mira 3 field emission electron microscope at the Department of Geology, Lund University. The quantitative determination of major elements was calculated from the energy peak-height ratio relative to standards, using AZtec software by Oxford Instruments.

Electron microprobe analysis

Electron microprobe/wavelength dispersive spectroscopy (EPMA/WDS) is an X-ray-based technique that is distinguished from the energy-dispersive because X-rays are 'dispersed' according to their wavelength using Bragg's reflection (Reed 1993). Each WDS detector is fit to collect X-rays dispersed within a specific wavelength range. Thus, the peak-to-background ratio is enhanced, and the resolution is better than with EDS detectors. The higher resolution of the WDS analysis enabled more accurate quantification of trace elements and REEs in the small-sized igneous zirconolite (preserved in one target rock in the ES, see paper IV). EPMA analyses were done using the JEOL JXA-8230 microanalyzer at the Universidad Nacional de Colombia.

Laser ablation inductively coupled mass spectrometry (LA-ICP-MS) for trace elements analysis

Differently from the scanning electron-based techniques, the LA-ICP-MS is a destructive method in which a high-energy laser is shot on the surface of a mineral and evaporates a sample fraction as an aerosol. The sample particles sweep from the cell to the plasma torch for ionization and are carried into the mass spectrometer. The elements are filtered according to their mass-charge ratio by quadrupoles. An ion counter collects the ion signals and yields a mass spectrum.

Trace element analysis of garnet was performed using the laser ablation inductively coupled plasma mass spectrometry (LA-ICP-MS) device at Lund University. The LA-ICP-MS system is equipped with a Teledyne Photon Machines G2 laser coupled to a Bruker Aurora Elite quadrupole. The instrument setup involved tuning and calibration of the ion masses of interest using the standard SRM NIST612 reference glass (Jochum et al. 2011). The configuration of the laser parameters and dwell time for data processing followed standard laboratory protocols.

U–Pb geochronology

U–Pb dating of zircon aimed to constrain the metamorphism, deformation and age of the igneous protolith in a syenodiorite within the Frontal wedge (paper III).

Cathodoluminescence imaging

Luminescence is produced in minerals by either crystal-structure defects or trace elements (Reed, 1993). The cathodoluminescence (CL) response occurs when electrons from an external source cause excitation in the energy levels of the atoms. This stimulation shifts electrons from the valence band to a normally empty conduction band, causing the emission of a photon.

A monochromatic CL detector linked to an SEM (Tescan Mira 3 used in this thesis) captures the photons within a wide wavelength spectrum of the visible region to generate a CL image. CL images of zircon can show details related to the crystal growth processes (Reed 1993; Corfu 2003). The CL images were used to characterize texturally different types of zircon in the studied rocks and for the selection of target areas for secondary ion microprobe U–Pb dating (SIMS).

U–Pb dating

U–Th–Pb geochronology is a common method for dating minerals and determining the age of high-temperature geological events (e.g., crystallization, magmatism, metamorphism). This dating method is based on the natural radioactive decay of uranium (U) and thorium (Th) to stable lead (Pb) isotopes. The two isotopes ^{238}U and ^{235}U produce ^{206}Pb and ^{207}Pb, respectively, and the ^{232}Th decays to ^{208}Pb. A fourth stable lead isotope, ^{204}Pb, may occur naturally in the structure of minerals and can be used to trace Pb background levels (see below). All three parent isotopes have a determined half-life ($t_{½}$) value, and the three decay systems have a decay constant (λ) that describes the disintegration rate of the radioactive nuclide.

Equation (4) expresses the relation between the daughter and parent isotopes, where D^* is the total number of the daughter (radiogenic) atoms at a given time,

D_0^* is the initial number of daughter atoms when the system closed, N is the content of parent atoms, and t is the time since the system closed (i.e., when the diffusion of parent and daughter atoms out of the crystal lattice ceased).

$$D^* = D^*_0 + N(e^{\lambda t} - 1) \quad (4)$$

In geological materials, the initial amount of radiogenic daughter (D^*_0) is unknown. For the U–Th–Pb system, this initial number is referred to as common Pb, which contains all four Pb isotopes in different proportions. The initial content of common Pb might be negligible in crystalline zircon and baddeleyite because the ion does not fit into the crystal lattice. However, fractions of common Pb may be accumulated in intracrystalline cracks, areas with radiation damage, or in inclusions of other phases.

To estimate the common Pb, the non-radiogenic Pb (i.e., ^{204}Pb) component is used as a proxy for the presence of common Pb, and radiogenic Pb isotopes are normalized to the measured ^{204}Pb. The radiogenic proportions present in the common-Pb are calculated assuming the evolution model of crustal Pb by Stacey and Kramers (1975) and subtracted from the measured radiogenic isotope.

Once the common Pb is corrected (if applicable), the age of the target mineral can be independently calculated for each of the three isotopic systems following the equations (5a–c), where the decay constants (λ) are known, and the isotopic ratios (^{206}Pb/^{238}U, ^{207}Pb/^{235}U, ^{208}Pb/^{232}Th) are measured by mass spectrometry.

$$^{206}Pb^* / {}^{238}U = e^{\lambda_{238} t} - 1 \quad (5a)$$

$$^{207}Pb^* / {}^{235}U = e^{\lambda_{235} t} - 1 \quad (5b)$$

$$^{208}Pb^* / {}^{232}Th = e^{\lambda_{232} t} - 1 \quad (5c)$$

The concordia is the result of equal ages obtained by two different systems, implying that the system remains closed and in equilibrium over time. If the resulting $t_{206/238}$ differs from $t_{207/235}$, the analysis is discordant. The discrepancy between the two isotopic systems may be caused by Pb-loss (open system and resetting), incorporation of common-Pb, or analysis in metamict domains (parts with crystalline lattice defects).

Secondary ion mass spectrometry (SIMS)

The development of the high-spatial-resolution in situ SIMS technique in the 1970s enabled measurements of the isotopic composition of microdomains in texturally complex solid materials. Secondary ion mass spectrometry (SIMS) is a powerful tool for high-precision dating using a very small volume of the sample (Ireland and Williams 2003). This analytical technique consists of a high-energy ion beam (i.e., O^-_2) that ablates small-diameter spots (7–40 mm) with a shallow pit depth (<4 mm) (Schoene 2013). The released material forms atomic ions or molecular ionic compounds and is accelerated into a mass spectrometer (op. cit.). An electrostatic analyzer filters the ionic compounds based on their kinetic energy. Then, the atomic ions are separated into ions of a low and high mass-to-charge ratio by a large-radius curve magnetic sector. Lastly, the target ions are collected by a system of electron multipliers and Faraday cups. The counts of each measured mass are corrected and normalized based on measurements of natural standards over the analytical session. The instrument used for geochronological dating was a CAMECA IMS 1280 located at the Swedish Museum of Natural History, Stockholm, following the analytical setup described by Whitehouse et al. (1997).

Summary of papers

The author statement of the papers compiled in this thesis is presented in Table 2.

Paper I

Urueña, C., Andersson, J., Möller, C., Lundgren, L., Göransson, M., Lindqvist, J. E., & Åkeson, U. (2021). *Variation in technical properties of granitic rocks with metamorphic conditions*. Engineering Geology, 293, 106283.

In this paper, we investigated how metamorphism during mountain building affects the technical properties of granitic aggregates. The production of crushed rock aggregates aims at rock materials that are highly resistant to mechanical abrasion and suitable for road and railroad construction. Due to the mineralogical, textural, and microstructural characteristics, granites are, in general, suitable for the production of high-performance aggregates.

Mountain building involves crustal deformation and metamorphism. These processes modify the petrographic characteristics of bedrock and influence the performance of crushed aggregates. The present study addresses a systematic investigation of the variation in the technical properties of granitic rocks that were metamorphosed during the syn- to late-collisional phase of the Sveconorwegian orogeny. The study was conducted along a 150-km profile across the Eastern Segment of the

Sveconorwegian Province. The bedrock shows differences in metamorphic recrystallization and deformation that reflect a metamorphic field gradient from low- to high-temperature conditions (from *c.* 550 to 800 °C).

For this study, the samples were classified into eight groups based on their macrostructural and petrographic characteristics. Two technical tests were used to measure the resistance to fragmentation and wear (cf. Methods section). Subsequently, the technical test results were combined with the quantitative and qualitative data on texture and mineralogy. Based on the technical test results, the samples are roughly classified into high- and low-performance aggregates.

Textural analysis showed that high grain boundary complexity and an uneven grain size distribution greatly improved the quality of the crushed rock aggregates. The rocks with the highest textural complexity and uneven grain-size distribution were recrystallized at relatively low temperatures (<600 °C) and under limited water availability. Rocks recrystallized at higher temperatures and under limited water availability also have high resistance to fragmentation and wear.

In contrast, rocks that recrystallized at high temperatures and hydrous conditions developed coarser grain sizes and smooth grain boundaries, resulting in low-performance aggregates. In particular, the technical properties are significantly affected by high-grade metamorphic recrystallization and extensive partial melting.

In granitic rocks, the modal proportions of rock-forming minerals show no correlation with the technical test values. Instead, the mode of recrystallization in feldspar and quartz influences to some extent, the performance of the aggregates. We identified that the occurrence of elongate quartz crystals and intergrowths of perthite and antiperthite correlates with optimal technical test values. In contrast to these, rock aggregates of low performance are characterized by tartan twinning in K-feldspar and albite twinning in plagioclase.

No single textural or mineralogical parameter could be identified as independent criterion for predicting aggregate functionality. Nonetheless, the relationships between the textures, mineral contents, and technical test values in this study demonstrate that temperature variations and the availability of hydrous fluids are the metamorphic factors that steer the technical properties of granitic aggregates in the studied area.

Paper II

Urueña, C., Möller, C., Andersson, J., Lindqvist, J. E., & Göransson, M. (2022). *The effect of metamorphism on the aggregate properties of gabbroic rocks*. Bulletin of Engineering Geology and the Environment 2022 81:5, 81(5), 1–27.

In this paper, we study the relationships between metamorphic conditions and aggregate functionality of metamorphosed gabbroic rocks. The bedrock in the Eastern Segment is predominantly granitic but also contains gabbroic components. In Sweden, aggregate production is concentrated on granitic rocks. However, the gabbroic components are part of crushed aggregates and can potentially boost or degrade the technical properties.

The studied rocks have low silica contents (SiO_2 44–49 %) and densities above 3.0 $g.cm^{-3}$. Due to mineralogical and compositional differences between granitic and gabbroic rocks, they respond differently to metamorphism. In general, the metamorphic mineral assemblage of a metagabbro is different from the igneous assemblage of its gabbro protolith, whilst the dominating process in granitic rocks is recrystallization of igneous quartz and feldspar.

Twenty-three samples of gabbroic rocks, from the same 150 km long profile in the Eastern Segment, were grouped according to the degree of recrystallization and the metamorphic conditions. Some metagabbroic rocks preserve progressive textural and mineral transformations over distances of only a few metres (or less). The degree of metamorphic recrystallization grades from incipient, in which igneous minerals are well-preserved, to complete. Migmatitic varieties of metagabbro were also included in the sample set.

The metagabbroic rocks vary widely in aggregate performance. Their functionality ranges from high-quality aggregates for road and railroad construction to aggregates unsuitable for use in any part of the construction. High resistance to fragmentation and wear correlates with the preservation of primary interlocking igneous gabbro texture in the rock with incipient metamorphic recrystallization. Metagabbros recrystallized at high temperatures and under limited hydration (i.e., pyroxene-bearing mafic granulites) also have good resistance to fragmentation but lower resistance to wear than the rocks with preserved igneous minerals. Metagabbros that have undergone complete metamorphic recrystallization under amphibolite-facies conditions (with or without partial melting) yielded poor technical test values and have low resistance to fragmentation and wear.

This study shows that the functionality of gabbroic rock aggregates is directly related to the character of metamorphic recrystallization. High metamorphic temperatures and high availability of water promoted coarsening of grain size, smoothening of grain boundaries, and partial melting (formation of leucosome). As in granitic rocks, these textural characteristics drastically reduce the resistance of the aggregates to fragmentation and wear.

The apparent relationships between the technical test values and the modal proportion of either hydrous (e.g., hornblende) or anhydrous minerals (e.g., pyroxene) ultimately reflect the role of hydrous fluids during

metamorphic recrystallization. This is shown by pyroxene-bearing metagabbros that recrystallized at high temperatures and low availability of H_2O conditions and yield high technical performance aggregates. The overall correlations presented in this study suggest that knowledge of the metamorphic conditions in a target area can allow prediction of aggregate performance.

Paper III

Urueña, C. and Möller, C. (*Manuscript*). *Fluid-induced metamorphism and deformation at the eastern boundary of the Sveconorwegian Province*

Deformation zones are important parts of orogens and their tectonometamorphic history. The Frontal wedge in the Eastern Segment is a steeply dipping N-S trending deformation zone that bounds the Sveconorwegian Province to the east. This study focuses on a case of metamorphic recrystallization in association with deformation and hydration within the Frontal wedge.

We investigated an occurrence of 1.2 Ga syenodiorite (locally grading to syenite) that exposes transitions from the undeformed, nearly pristine, igneous protolith to strongly deformed and fully recrystallized varieties. The coarse-grained syenitoid rock was heterogeneously deformed and largely recrystallized to protomylonite and mylonite; near-pristine igneous rocks are only locally preserved. The variation in degree of metamorphic recrystallization is closely related to the state of deformation.

The igneous phases in the well-preserved rock are mesoperthite, plagioclase, orthopyroxene, and minor clinopyroxene and biotite. The metamorphic assemblage in the deformed rocks consists of plagioclase (oligoclase and albite), biotite, quartz, garnet, clinozoisite, titanite, and subordinate K-feldspar. The nearly anhydrous igneous mineral assemblage in the near-pristine rock and the hydrated metamorphic assemblage, which includes biotite and clinozoisite, suggest that metamorphic reactions were associated with the introduction of a hydrous fluid. Thermobarometric estimates, using Average PT (thermocalc) and winTWQ, suggest equilibrium at 540–600 °C, 9–12 kbar, and a_{H2O}= 0.6–0.8. The estimates of a_{H2O} suggest that, although hydrous fluids were introduced, the high-strain domains were still not fully water-saturated.

The field relations suggest that the hydrous fluid was introduced through deformation zones (brittle or ductile). The effects of the limited availability of hydrous fluid are also reflected in the variations in the distribution of REE in the garnet and variable Al^{3+} vs. Fe^{3+} in clinozoisite in different microdomains. These variations in mineral chemistry show that full chemical equilibrium was attained only at the microscale.

The presence of baddeleyite and small amounts of zirconolite, both Zr-bearing igneous minerals, and metamorphic zircon offered dating of igneous and tectonometamorphic events, respectively. U–Pb analysis of zircon dated the magmatic crystallization of the syenodiorite at 1230 ± 2 Ma. The small metamorphic zircon crystals gave a Sveconorwegian imprecise age of the metamorphic recrystallization around 1Ga.

Paper IV

Urueña, C., Möller, C., Plan, A. (*Manuscript*). *Metamorphic titanite–zircon pseudomorphs after igneous zirconolite.*

This paper reports on the occurrence of metamorphic titanite + zircon pseudomorphs after zirconolite. The pseudomorphs were found in a variably deformed and recrystallized 1.2 Ga syenite and syenodiorite (studied also in paper III). We used backscatter electron and cathodoluminescence imaging to document the textural relationships of zircon and other Zr-bearing phases.

Typically, titanite + zircon intergrowths are elongated or platy titanite crystals speckled with micron-sized zircon inclusions. In places, the intergrowths have a subrounded shape and are very fine multi-nuclei aggregates of polycrystalline zircon intergrown with titanite. Commonly, these intergrowths are closely related to epidote, either that epidote crystals form around or as part of the intergrowth. In general, all intergrowths are smaller than 15 microns. Monomineralic polycrystalline aggregates of zircon, up to 20 μm in size, are common in these recrystallized rocks.

The undeformed and near-pristine syenodiorite preserves igneous baddeleyite and zirconolite crystals. Occasionally, baddeleyite crystals are rimmed by thin coronas of polycrystalline zircon. Based on the textural relationships, we interpret that titanite + zircon intergrowths formed from the metamorphic breakdown of zirconolite and the monomineralic polycrystalline zircon aggregates formed at the expense of baddeleyite.

The metamorphic reaction for the formation of metamorphic titanite + zircon intergrowths requires the release of silica and calcium from the consumption of igneous pyroxene and feldspars. As a result, the SiO_2 and CaO reacted with zirconolite to produce metamorphic titanite and zircon. In a previous study (paper III), we showed that the metamorphic reactions in the syenodiorite took place at high-pressure epidote-amphibolite facies conditions during deformation and introduction of hydrous fluid. The findings in this study confirm that metamorphic zircon formed under subsolidus conditions from igneous Zr-bearing minerals, mainly baddeleyite, and that aqueous fluids promoted element mobility.

Table 2. Author contributions to papers included in this thesis. *Italics*: not co-author of the paper. **Bold**: main authors. * = Supervision.

	Paper I	Paper II	Paper III	Paper IV
Study design	C. Möller J. Andersson J.E. Lindqvist M. Göransson U. Åkesson	C. Möller J. Andersson	C. Möller C. Urueña	C. Urueña C. Möller
Field documentation and sampling	J. Andersson C. Möller C. Urueña M. Göransson L. Lundgren	C. Möller C. Urueña J. Andersson M. Göransson	C. Möller C. Urueña	-
Bulk geochemical measurements	Purchased + SGU data	Purchased	Purchased + SGU data	-
Rock technical measurements (LA and M_{DE})	Purchased (SGU) + SGU data	Purchased (SGU) + Scandinavian Stone data	-	-
Thin section manufacturing	Purchased	Purchased	Purchased	Purchased
Petrographic textural analysis	C. Möller C. Urueña J. Andersson J.E. Lindqvist	C. Möller C. Urueña J. Andersson	C. Möller C. Urueña	C. Urueña C. Möller
Quantitative petrographic measurements	C. Urueña J.E. Lindqvist*	C. Urueña	-	-
SEM textural documentation	-	-	C. Urueña	C. Urueña C. Möller*
EDS mineral chemical analysis	C. Urueña C. Möller*	C. Urueña	C. Urueña	C. Urueña
WDS mineral chemical analysis				*M. Arrieta* (UN)
Geothermobarometric calculations			C. Urueña C. Möller*	
EBSD analysis				A. Plan
Zircon separation			C. Urueña *L. Johansson** (LU)	
SIMS U-Pb isotope analysis of zircon			C. Urueña *H. Jeon** (NordSIMS)	
SIMS trace element analysis of zircon			C. Urueña *H. Jeon** (NordSIMS)	
SIMS data reduction			*M. Whitehouse* (NordSIMS)	
LA-ICP-MS trace element analysis of garnet			C. Urueña *T. Naeraa** (LU)	
LA-ICP-MS data reduction			*T. Naeraa* (LU)	
Photographic illustrations	C. Möller C. Urueña	C. Möller C. Urueña	C. Urueña C. Möller	C. Urueña C. Möller
Data plots /diagrams	C. Urueña	C. Urueña	C. Urueña	C. Urueña A. Plan
Other artwork (maps, conceptual sketches)	C. Urueña C. Möller	C. Urueña C. Möller	C. Urueña C. Möller	C. Urueña
Tables	C. Urueña C. Möller	C. Urueña C. Möller	C. Urueña C. Möller	C. Urueña
Data interpretation and discussion	J. Andersson C. Möller C. Urueña J.E. Lindqvist M. Göransson	C. Möller J. Andersson C. Urueña	C. Möller C. Urueña	C. Urueña C. Möller

Manuscript writing				
Writing: original draft	C. Urueña	C. Urueña	C. Urueña	C. Urueña
Writing: review and editing	**C. Möller** **J. Andersson** **C. Urueña** J.E. Lindqvist M. Göransson U. Åkeson	**C. Möller** **C. Urueña** **J. Andersson** J.E. Lindqvist M. Göransson	**C. Möller** **C. Urueña**	**C. Urueña** **C. Möller** A. Plan

Conclusions and implications

The effect of metamorphic processes on rock technical properties

The systematic variations in technical properties of felsic and mafic rocks in the Eastern Segment of the Sveconorwegian Province are steered by the mode of metamorphic recrystallization. The different states of recrystallization stemmed primarily from variations in the metamorphic temperature and the availability of hydrous fluids.

Recrystallization at low and high temperatures under H_2O-undersaturated conditions resulted in the development of complex textures. These textures are characterized by an uneven grain size distribution with a large proportion of very fine-grained crystals, irregular grain boundaries, mineral intergrowths or exsolutions, coronitic textures, and/or relict igneous textures. The complex textures improve the resistance of rock aggregates to fragmentation and wear.

In contrast, high-temperature conditions and high availability of hydrous fluids enhance the crystal growth, production of regular crystal shapes, mineral reactions, and partial melting. Consequently, the recrystallization produces less complex or straight grain boundaries; for example, within granoblastic mineral aggregates, which negatively affect the resistance to fragmentation and wear. The rock aggregates with the lowest performance correlate to even-grained textures, coarser grain sizes, and smooth grain boundaries.

The influence of mineralogy on the technical properties is secondary to the textural aspects in both granitic and gabbroic rocks. The mineral arrangement of laminar and planar minerals, such as biotite and amphibole, has a greater impact on reducing the resistance to mechanical abrasion than their respective modal content. Similarly, the mode of recrystallization of quartz and feldspar is significantly more important than their modal proportions.

In summary, the textural and microstructural parameters that steer the technical properties are determined dominantly by temperature- and fluid-dependent processes. Therefore, the functionality of rock aggregates can be inferred from a general knowledge of the metamorphic history of the bedrock. Following the correlations between metamorphic conditions and technical properties in the Eastern Segment, further studies on bedrock aggregates can be conducted in metamorphic basements in different tectonic settings.

Metamorphic recrystallization at deep crustal levels within the easternmost boundary of the Sveconorwegian Province

Metamorphic recrystallization and mineral reactions within the basement at the eastern boundary of the Sveconorwegian Province were controlled by deformation and the infiltration of hydrous fluid. An investigated locality at Näsbyholm exposes syenodiorite and subordinate syenite with progressive transitions from undeformed igneous rocks to fully recrystallized mylonites. In weakly recrystallized varieties, igneous minerals are partly preserved as metastable relicts within the incompletely metamorphosed rock; such mineral relationships indicate a 'frozen-in' recrystallization process.

In deformed rocks, most igneous minerals have been recrystallized to a metamorphic assemblage consisting of plagioclase, biotite, quartz, garnet, and epidote. The breakdown of igneous pyroxene and feldspar produced metamorphic minerals and released SiO_2. The silica reacted with Zr-bearing oxides to form metamorphic zircon.

The metamorphic zircon-forming reactions are supported by microtextures. Replacement textures include polycrystalline zircon rimming baddeleyite crystals and intergrowths of titanite and zircon as pseudomorphs after zirconolite. Although the polycrystalline nature and small size of zircons hampered precise age determination, U–Pb SIMS-dating of metamorphic zircon grains gave an imprecise Sveconorwegian age.

Svensk sammanfattning

Berggrunden i sydvästra Skandinavien utgörs till största delen av den Svekonorvegiska Provinsen, rötterna av en bergskedja som fanns för 1070–920 miljoner år sedan. Denna bergskedja var en del av ett större tektoniskt sammanhang: bildningen av superkontinenten Rodinia. Östra Segmentet, som är den östligaste delen av den Svekonorvegiska Provinsen, trycktes djupt ner, in under den västliga delen av den Svekonorvegiska bergskedjan, och genomgick metamorfos vid 35-40 km djup och höga tryck, ~10 kbar. Under denna metamorfa händelse värmdes berggrunden upp till höga temperaturer i de västra delarna av Östra Segmentet (~800 °C), högre än i de östra delarna (<600 °C). Denna skillnad i temperatur under metamorfosen är den huvudsakliga orsaken till variationer i mineralparageneser och texturer i bergarterna inom Östra Segmentet. En annan anledning är lokala skillnader i tillgång till vattenrika lösningar i berggrunden.

Huvudsyftet med de två första undersökningarna i denna avhandling har varit att klarlägga hur tekniska egenskaper för krossbergsballast (makadam) varierar med de geologiska förhållandena då berggrunden genomgick metamorfos. Krossat bergmaterial används i stora mängder i samhället (i Sverige drygt ett kilo per invånare och timme): vid byggnation och underhåll av väg och järnväg, för produktion av betong, som fyllnadsmaterial, m.m. Bergmaterialets tekniska egenskaper är avgörande för hur det kan användas. Egenskaper som vanligen testas är motstånd mot fragmentering (mäts i Los Angeles-värde, LA) och motstånd mot abrasion (Micro DeVal-värde, M_{DE}); för båda testerna motsvarar låga värden goda motståndsegenskaper. Östra Segmentet är väl lämpat för undersökning av hur olika metamorfa förhållanden påverkar bergets tekniska egenskaper eftersom området består av bergarter av samma ursprung och lika kemiska sammansättningar och metamorf temperatur dessutom varierar systematiskt. Om samband mellan olika geologiska processer och/eller miljöer och bergkvalitet går att klarlägga finns potential att även i andra områden kunna förutse bergmaterials egenskaper utifrån geologiska förhållanden.

Provtagning av felsiska och basiska bergarter (70–80 kg per prov) genomfördes längs en ~30 km bred och ~150 km lång profil över Östra Segmentet, från Vrigstad i öster till Varberg i väster. Proven testades med avseeende på tekniska egenskaper och jämfördes med resultaten av geokemisk, petrofysisk och petrografisk analys. Resultaten visar att de tekniska egenskaperna för granitiska bergarter (38 prov) styrs av mikrotexturernas komplexitet i bergarternas kvarts- och fältspat-aggregat. Skillnaderna i mikrotextur beror på att rekristallisionsmekanismer i mineral varierar med metamorfa förhållanden. Metamorf temperatur och tillgång till vatten identifierades som två kritiska variabler; låga temperaturer och "torra" förhållanden gynnar båda bildningen av komplexa mikrotexturer och därmed goda tekniska egenskaper. Biotithalten i de grantiska bergarterna är genomgående låg (<20%) och har ingen betydelse. Punkträkning av mineral kan därmed inte användas för prediktion av tekniska egenskaper för dessa bergarter. De tekniska egenskaperna för gabbrobergarter (23 prov) längs samma profil varierar med textur, mineral och kornstorlek. Studien bekräftade att även för gabbrobergarter är metamorf temperatur och tillgång till vatten kritiska faktorer. Metamorfos under "torra" förhållanden och ofullständig omkristallisation korrelerar båda med goda tekniska egenskaper. Bäst värden erhölls för bergarter med välbevarad subofitisk textur och sämst för grovkorniga och/eller migmatitiska amfiboliter. Testvärdena var sämst för migmatitiska bergarter i vilka leukosomet (den ljusa smältfasen/ådrorna) har isotrop textur, dvs. då bergarten inte har deformerats efter leukosomets kristallisation (för både granitiska och basiska bergarter). Det finns goda möjligheter att förutse tekniska egenskaper i fält eftersom en del bergartstexturer och strukturer är makroskopiska, exempelvis mängden leukosom, leukosomets textur, samt bevarandegrad av ofitisk eller subofitisk textur i gabbrobergarter.

Avhandlingens tredje studie syftade till att dokumentera karaktären av metamorf omkristallisation i den östliga, vertikalt stupande och 20 km breda deformationszonen i Östra Segmentet, vilken vanligen anses som den östliga gränsen för den Svekonorvegiska Provinsen. Målet var att, om möjligt, åldersbestämma metamorfosen med U–Pb datering av metamorf zirkon. För detta syfte dokumenterades och provtogs en syenodioritisk bergart i Näsbyholm öster om Värnamo. På enstaka ställen, där bergarten inte har påverkats av deformation, har den en välbevarad grovkornig magmatisk textur och delvis välbevarade magmatiska mineral. Den magmatiska paragenesen består av plagioklas, alkalifältspat, ortopyroxen och mindre mängder ilmenit, biotit, apatit och klinoyroxen. Med undantag av en mycket liten mängd biotit består bergarten av icke-hydrerade mineral. Där bergarten har deformerats har den omkristalliserats till en metamorf paragenes som består av plagioklas (oligoklas och albit), biotit, kvarts, titanit, epidotmineral (klinozoisit och epidot) och mindre mängder kalifältspat och granat; paragenesen är typisk för metamorfos i epidot–amfibolit-facies, dvs. temperaturer ≤600 °C. Den metamorfa bildningen av biotit, klinozoisit och epidot kräver tillförsel av H_2O (från en vattenförande lösning). Termobarometriska beräkningar indikerar att de metamorfa mineralen bildades vid 540–600 °C och 9–12 kbar, dvs. vid 35–45 km djup. U–Pb-datering av magmatisk zirkon och baddeleyit gav åldern 1230 ± 6

miljoner år för magmatisk kristallisation av den syenodioritiska intrusivbergarten. Små metamorfa zirkonkristaller (*c*. 20 mikrometer stora) gav oprecisa åldersresultat runt 1000 miljoner år. Studien visar ett exempel på att metamorf omkristallisation styrdes av deformation och infiltration av vattenförande lösningar, även på stort djup, i den östliga deformationszonen i den Svekonorvegiska Provinsen.

Den fjärde studien är en elektronmikoskopi-baserad dokumentation av små (*c*.15 mikrometer) aggregat av titanit+zirkon i syenodiorit. Dessa titanit+zirkon-aggregat är sannolikt pseudomorfer efter det ovanliga mineralet zirkonolit, $CaZrTi_2O_7$. Få och endast några mikron stora rester av zirkonolit hittades i bergarten. De två största zirkonolitkristallerna (8 resp. 12 mikrometer) analyserades med mikrosond. Bildningen av titanit+zirkon-pseudomorfer efter zirkonolit är en parallell till bildningen av metamorf polykristallin zirkon, $ZrSiO_4$, efter magmatisk baddeleyit, ZrO_2. För båda reaktionerna krävs att SiO_2 tillförs från andra metamorfa reaktioner i bergarten. För bildning av titanit+zirkon krävs utöver detta att CaO tillförs från nedbrytningen av magmatisk anortitförande plagioklas, vilket kan ske i samband bildningen av metamorf albit och oligoklas.

Popular summary

Earth's historical record is full of cycles of uplift and decline of mountain ranges. Mountains are formed by slow movements of large portions of Earth's crust (i.e., tectonic plates). At times, these plates collide with each other, pushing the rock upward and increasing temperature and pressure. The rock at the surface weakens, and the underlying rock deforms, changes its composition, and even melts if the temperature is high enough. This geological process that transforms rocks is called metamorphism. When the pushing forces cease, the mountain range collapses due to the mass imbalance of the piled-up rock. Atmospheric factors (e.g., air currents, water runoff, ice sliding) then act to erode the rock surface. In the final phase of a mountain cycle, the deep roots that once supported the mountain belt may reach the Earth's surface.

The metamorphic process involves the breakdown, replacement, and recrystallization of minerals. Studying the relationships among coexistent minerals that make up rocks sheds light on how, when, and under what conditions the rocks were modified. This metamorphic history is recorded by the minerals and their characteristics, such as size, shape, arrangement, and chemical composition. This group of characteristics is called rock texture. Curiously, these same textural characteristics also determine the rock's resistance as a construction material.

Crushed rock aggregates are an alternative to sand and gravel used in road and railroad construction. However, rock aggregates must have favourable mechanical properties. High resistance to fragmentation and wear ensures that the material is suitable and durable. In addition, efficient production of high-quality material reduces cost overruns due to overexploitation and, consequently, the environmental impacts.

Most rocks in Sweden have been metamorphosed and deformed in various ways during mountain building. Therefore, their mechanical properties are highly variable. This thesis looks into the metamorphic process in the deep roots of an ancient mountain belt in southwestern Sweden and its effects on the technical properties of the rocks.

A continental crustal portion, known as the Eastern Segment, was deeply buried and metamorphosed during the mountain-building event known as the Sveconorwegian orogeny 1000 Ma ago. The rocks of the Eastern Segment show progressive changes in the state of recrystallization, reflecting variations in temperature and availability of water during metamorphism.

For this investigation, rocks in various metamorphic states were collected across the Eastern Segment. These were then observed under a microscope to analyse variations in mineral relationships, composition, and texture. In addition, technical laboratory tests were carried out to measure the resistance of rocks to fragmentation and wear.

The results indicate that irregular grain shapes, intricate grain boundaries, and a high proportion of fine grain sizes boost the resistance to fragmentation. But what factors influence these characteristics? Correlation with metamorphic conditions suggests that rocks with such textural features recrystallized at low or very high temperatures but always in the absence of water. Water enables the formation of new minerals and causes the rocks to melt at high temperatures. Likewise, the temperature rise promotes the growth of minerals and the reorganization of their structures, producing more regular shapes. Some parts of the Eastern Segment that were partially molten during metamorphism developed well-shaped grains and

coarser grain-size textures. These characteristics resulted in a drastic reduction of the resistance to wear.

This study also includes findings on metamorphic processes at deep levels of the crust at the easternmost boundary of the Sveconorwegian orogen. Even though rocks in the eastern boundary are only weakly deformed and have minor mineral changes, a progressive transformation of primary minerals into metamorphic minerals is observed in some rocks. This gradual recrystallization relied on the amount of infiltrated water. Thus, in places with low water infiltration, mineral reactions were incomplete, leaving remnants of old minerals that were partially replaced by metamorphic minerals. In places with higher water infiltration, the rocks were strongly deformed, and old minerals were completely replaced. These relationships between primary minerals and metamorphic products reflect fluid-rock interactions and how the fluid dynamics steered the metamorphic evolution of the Eastern Segment during mountain-building.

Resumen de divulgación científica

El registro histórico de la Tierra está lleno de ciclos de levantamiento y destrucción de cadenas montañosas. Las montañas se forman por movimientos lentos de grandes porciones de la corteza terrestre (es decir placas tectónicas). A veces estas placas chocan entre sí, lo que empuja rocas hacia arriba y aumenta la temperatura y la presión. Las rocas en la superficie se debilitan y las rocas que yacen por debajo se deforman, cambian su composición, e incluso se funden cuando la temperatura es lo suficientemente alta. Este proceso geológico que transforma las rocas se llama metamorfismo. Cuando cesan las fuerzas de empuje, la cadena montañosa colapsa debido al desequilibrio de masa de la roca apilada. Entonces, los factores atmosféricos (corrientes de aire y agua, deslizamientos o remoción de hielo) actúan erosionando la superficie rocosa. En la fase final del ciclo de una cadena montañosa, las raíces profundas que una vez la sostuvieron pueden llegar a la superficie terrestre.

El proceso metamórfico implica la descomposición, reemplazo y recristalización de minerales. El estudio de las relaciones entre minerales coexistentes que componen las rocas nos da información sobre cómo, cuándo y en qué condiciones se modificaron dichas rocas. Esa historia geológica queda registrada en las características de los minerales tales como el tamaño, la forma, su organización y su composición química. Este conjunto de características se denomina textura de la roca. Curiosamente, estas mismas características texturales también determinan la capacidad de resistencia de una roca como material de construcción.

Los agregados de roca triturada son una alternativa a la arena y grava usadas en la construcción de carreteras y vías férreas. Sin embargo, los agregados de roca deben tener propiedades mecánicas favorables. Una alta resistencia a la fragmentación y a la abrasión asegura que el material es apropiado y duradero. Además, la producción eficiente de materiales de alta calidad reduce sobrecostos por sobreexplotación y, consecuentemente, se reduce el impacto ambiental.

La mayoría de rocas en Suecia han sido metamorfoseadas y deformadas de varias maneras durante procesos de formación de montañas. Por lo tanto, las propiedades mecánicas de las rocas son ampliamente variables. Esta tesis examina el proceso de metamorfismo en las raíces profundas de un antiguo cinturón montañoso en el suroccidente de Suecia y sus efectos en las propiedades técnicas de las rocas.

Una porción de corteza continental, llamada Segmento Oriental, fue profundamente enterrada y metamorfoseada durante el evento de formación de montañas, conocido como Orogenia Sueco–Noruega, hace1000 millones de años. Las rocas del Segmento Oriental muestran cambios progresivos en el estado de recristalización, que reflejan variaciones en la temperatura y la disponibilidad de agua durante el metamorfismo.

Para esta investigación se colectaron rocas a lo largo del Segmento Oriental con diferente grado de metamorfismo. Luego, estas rocas fueron observadas bajo el microscopio para analizar variaciones en las relaciones minerales, composición y textura. Además, se realizaron pruebas técnicas de laboratorio para medir la resistencia a la fragmentación y abrasión.

Los resultados señalan que formas de grano irregulares, con contactos intrincados entre granos y una alta proporción de tamaños de grano fino aumentan la resistencia a la fragmentación. Pero ¿qué factores influencian las características texturales? La correlación con las condiciones de metamorfismo indica que rocas con estas características texturales recristalizaron a bajas o muy altas temperaturas,

pero siempre en ausencia de agua como fluido libre. El agua facilita la formación de nuevos minerales y conlleva a la fusión de las rocas en condiciones de alta temperatura. Así mismo, el aumento de temperatura promueve el crecimiento de minerales y la reorganización de su estructura, creando formas más regulares. Algunas partes del Segmento Oriental que fueron parcialmente fundidas durante el metamorfismo desarrollaron texturas con cristales bien formados y de tamaño más grueso. Estas características resultaron en una reducción drástica de la resistencia al desgaste mecánico.

Esta investigación también incluye hallazgos de los procesos metamórficos en la corteza profunda en el borde más oriental del orógeno Sueco–noruego. Si bien, las rocas del margen oriental están débilmente deformadas y con cambios minerales menores, en algunas rocas se observa la transformación progresiva de minerales primarios a minerales metamórficos. Esta recristalización paulatina estuvo controlada por la cantidad de infiltración de agua. De forma que, en aquellos lugares con poca infiltración de agua, las reacciones minerales fueron incompletas, dejando remanentes de los antiguos minerales parcialmente reemplazados por minerales metamórficos. En lugares donde la infiltración de agua fue mayor, las rocas están fuertemente deformadas y los minerales antiguos fueron completamente reemplazados. Estas relaciones entre minerales primarios y productos metamórficos reflejan las interacciones fluido-roca, y cómo la dinámica del fluido controló la evolución metamórfica del Segmento Oriental durante el evento de formación de montañas.

REFERENCES

Afolagboye, L. O., Talabi, A. O., and Akinola, O. O. (2016). Evaluation of selected basement complex rocks from Ado-Ekiti, SW Nigeria, as source of road construction aggregates. *Bulletin of Engineering Geology and the Environment, 75*(2), 853–865. https://doi.org/10.1007/S10064-015-0766-1/TABLES/3

Åkesson, U., Lindqvist, J. E., Göransson, M., and Stigh, J. (2001). Relationship between texture and mechanical properties of granites, central Sweden, by use of image-analysing techniques. *Bulletin of Engineering Geology and the Environment, 60,* 277–284. https://doi.org/10.1007/s100640100105

Åkesson, U., Stigha, J., Lindqvist, J. E., and Göransson, M. (2003). The influence of foliation on the fragility of granitic rocks, image analysis and quantitative microscopy. *Engineering Geology, 68*, 275–288. https://doi.org/10.1016/S0013-7952(02)00233-8

Andersson, J., Söderlund, U., Cornell, D., Johansson, L., and Möller, C. (1999). Sveconorwegian (-Grenvillian) deformation, metamorphism and leucosome formation in SW Sweden, SW Baltic Shield: Constraints from a Mesoproterozoic granite intrusion. *Precambrian Research, 98*(1–2), 151–171. https://doi.org/10.1016/S0301-9268(99)00048-0

Andersson, J., Möller, C., and Johansson, L. (2002). Zircon geochronology of migmatite gneisses along the Mylonite Zone (S Sweden): a major Sveconorwegian terrane boundary in the Baltic Shield. *Precambrian Research, 114*(1–2), 121–147. https://doi.org/10.1016/S0301-9268(01)00220-0

Andréasson, P. G., and Dallmeyer, R. D. (1995). Tectonothermal evolution of high-alumina rocks within the Protogine Zone, southern Sweden. *Journal of Metamorphic Geology, 13*(4), 461–474. https://doi.org/10.1111/J.1525-1314.1995.TB00234.X

Austin-Hegart, E., Cornell, D., Hellström, F. A., and Lundqvist, I. (2007). Emplacement ages of the mid-Proterozoic Kungsbacka Bimodal Suite, SW Sweden. *GFF, 129*(3), 227–234. https://doi.org/10.1080/11035890701293227

Beckman, V., Möller, C., Söderlund, U., and Andersson, J. (2017). Zircon growth during progressive recrystallization of Gabbro to Garnet Amphibolite, Eastern Segment, Sveconorwegian orogen. *Journal of Petrology, 58*(1), 167–188. https://doi.org/10.1093/petrology/egx009

Best, M. G. (2003). *Igneous and Metamorphic Petrology* (Second ed.). Blackwell https://doi.org/10.1180/minmag.1983.047.344.33

Bingen, B., Nordgulen, Ø., and Viola, G. (2008). A four-phase model for the Sveconorwegian orogeny, SW Scandinavia. *Norwegian Journal of Geology, 88*, 43–72.

Bingen, B., Viola, G., Möller, C., Auwera, J. V., Laurent, A., and Yi, K. (2021). The Sveconorwegian orogeny. *Gondwana Research, 90*, 273–313. https://doi.org/10.1016/j.gr.2020.10.014

Brander, L., and Söderlund, U. (2009). Mesoproterozoic (1.47–1.44 Ga) orogenic magmatism in Fennoscandia; Baddeleyite U–Pb dating of a suite of massif-type anorthosite in S. Sweden. *International Journal of Earth Sciences, 98*(3), 499–516. https://doi.org/10.1007/S00531-007-0281-0

Brander, L., Appelquist, K., Cornell, D., and Andersson, U. B. (2011). Igneous and metamorphic geochronologic evolution of granitoids in the central Eastern Segment, southern Sweden. *International Geology Review, 54*(5), 509–546. https://doi.org/10.1080/00206814.2010.543785

Brattli, B. (1992). The influence of geological factors on the mechanical properties of basic igneous rocks used as road surface aggregates. *Engineering Geology, 33*(1), 31–44. https://doi.org/10.1016/0013-7952(92)90033-U

Christoffel, C. A., Connelly, J. N., and Åhäll, K. I. (1999). Timing and characterization of recurrent pre-Sveconorwegian metamorphism and deformation in the Varberg-Halmstad region of SW Sweden. *Precambrian Research, 98*(3–4), 173–195. https://doi.org/10.1016/S0301-9268(99)00046-7

Coint, N., Slagstad, T., Roberts, N. M. W., Marker, M., Røhr, T., and Sørensen, B. E. (2015). The Late Mesoproterozoic Sirdal Magmatic Belt, SW Norway: Relationships between magmatism and metamorphism and implications for Sveconorwegian orogenesis. *Precambrian Research, 265*, 57–77. https://doi.org/10.1016/J.PRECAMRES.2015.05.002

Corfu, F. (2003). Atlas of Zircon Textures. *Reviews in Mineralogy and Geochemistry, 53*(1), 469–500. https://doi.org/10.2113/0530469

Engvik, A. K., Bingen, B., and Solli, A. (2016). Localized occurrences of granulite: P–T modeling, U–Pb geochronology and distribution of early-Sveconorwegian high-grade metamorphism in Bamble, South Norway. *Lithos, 240–243*, 84–103. https://doi.org/10.1016/J.LITHOS.2015.11.005

Ersoy, A., and Waller, M. D. (1995). Textural characterisation of rocks. *Engineering Geology, 39*(3–4), 123–136. https://doi.org/10.1016/0013-7952(95)00005-Z

Fossen, H. (2010). *Structural geology*. Cambridge University Press.

Gomez-Rivas, E., Butler, R. W. H., Healy, D., and Alsop, I. (2020). From hot to cold - The temperature dependence on rock deformation processes: An introduction. *Journal of Structural Geology, 132*, 103977. https://doi.org/10.1016/J.JSG.2020.103977

Gong, Z., Evans, D. A. D., Elming, S. Å., Söderlund, U., and Salminen, J. M. (2018). Paleomagnetism, magnetic anisotropy and U-Pb baddeleyite geochronology of the early Neoproterozoic Blekinge-Dalarna dolerite dykes, Sweden. *Precambrian Research, 317*, 14–32. https://doi.org/10.1016/J.PRECAMRES.2018.08.019

Göransson, M. (2018). *MinBaS Innovation Mineral-Ballast-Sten Insatsområde 1 Rapport nr 2014-04347*.

Göransson, M., Persson, L., and Wahlgren, C. H. (2004). The variation of bedrock quality with increasing ductile deformation. *Bulletin of Engineering Geology and the Environment, 63*(4), 337–344. https://doi.org/10.1007/s10064-004-0248-3

Hansen, E., Johansson, L., Andersson, J., LaBarge, L., Harlov, D., Möller, C., and Vincent, S. (2015). Partial melting in amphibolites in a deep section of the Sveconorwegian Orogen, SW Sweden. *Lithos, 236–237*, 27–45. https://doi.org/10.1016/j.lithos.2015.08.010

Hellman, F., Åkesson, U., and Eliasson, T. (2011). *Kvantitativ petrografisk analys av bergmaterialen metodbeskrivning. VTI rapport 714.*

Higgins, M. D. (2006). *Quantitative Textural Measurements in Igneous and Metamorphic Petrology*. Cambridge University Press. https://doi.org/10.1017/CBO9780511535574

Hoffman, P. F. (1988). United Plates of America, The Birth of a Craton: Early Proterozoic Assembly and Growth of Laurentia. *Ann. Rev. Earth Plan-*

et. Sci, 16, 543–603. https://doi.org/10.1146/ANNUREV.EA.16.050188.002551

Holness, M. B. (2008). Decoding migmatite microstructures. In E. W. Sawyer and M. Brown (Eds.), *Working with migmatites* (Short Course, pp. 57–76). Mineralogical Association of Canada.

Hubbard, F. H. (1975). The Precambrian crystalline complex of south-western Sweden. The geology and petrogenetic development of the Varberg region. *GFF, 97*(3), 223–236.

Hubbard, F. H. (1989). The geochemistry of Proterozoic lower-crustal depletion in southwest Sweden. *Lithos, 23*(1–2), 101–113. https://doi.org/10.1016/0024-4937(89)90025-X

Ireland, T. R., and Williams, I. S. (2003). Considerations in Zircon Geochronology by SIMS. *Reviews in Mineralogy and Geochemistry, 53*(1), 215–241. https://doi.org/10.2113/0530215

Jarl, L. G. (2002). U-Pb zircon ages from the Vaggeryd syenite and the adjacent Hagshult granite, southern Sweden. *GFF, 124*(4), 211–216. https://doi.org/10.1080/11035890201244211

Jochum, K. P., Weis, U., Stoll, B., Kuzmin, D., Yang, Q., Raczek, I., Jacob, D. E., Stracke, A., Birbaum, K., Frick, D. A., Günther, D., and Enzweiler, J. (2011). Determination of Reference Values for NIST SRM 610–617 Glasses Following ISO *Guidelines. Geostandards and Geoanalytical Research, 35*(4), 397–429. https://doi.org/10.1111/J.1751-908X.2011.00120.X

Johansson, Å. (2021). Cleaning up the record – revised U-Pb zircon ages and new Hf isotope data from southern Sweden. *GFF, 143*(4), 328–359. https://doi.org/10.1080/11035897.2021.1939777

Johansson, L., Lindh, A., and Möller, C. (1991). Late Sveconorwegian (Grenville) high-pressure granulite facies metamorphism in southwest Sweden. *Journal of Metamorphic Geology, 9*(3), 283–292. https://doi.org/10.1111/j.1525-1314.1991.tb00523.x

Kulakov, E. V., Slagstad, T., Ganerød, M., and Torsvik, T. H. (2022). Paleomagnetism and 40Ar/39Ar geochronology of Meso-Neoproterozoic rocks from southwest Norway. Implications for magnetic remanence ages and the paleogeography of Baltica in a Rodinia supercontinent context. *Precambrian Research, 379*, 106786. https://doi.org/10.1016/J.PRECAMRES.2022.106786

Larsson, D., and Söderlund, U. (2005). Lu–Hf apatite geochronology of mafic cumulates: An example from a Fe–Ti mineralization at Smålands Taberg, southern Sweden. *Chemical Geology, 224*(4), 201–211. https://doi.org/10.1016/J.CHEMGEO.2005.07.007

Li, Z. X., Bogdanova, S. V., Collins, A. S., Davidson, A., De Waele, B., Ernst, R. E., Fitzsimons, I. C. W., Fuck, R. A., Gladkochub, D. P., Jacobs, J., Karlstrom, K. E., Lu, S., Natapov, L. M., Pease, V., Pisarevsky, S. A., Thrane, K., and Vernikovsky, V. (2008). Assembly, configuration, and break-up history of Rodinia: A synthesis. *Precambrian Research, 160*(1–2), 179–210. https://doi.org/10.1016/j.precamres.2007.04.021

Lindqvist, J. E., Åkesson, U., and Malaga, K. (2007). Microstructure and functional properties of rock materials. *Materials Characterization, 58*(11–12), 1183–1188. https://doi.org/10.1016/J.MATCHAR.2007.04.012

Lundqvist, S., and Göransson, M. (2001). *Evaluation and Interpretation of Microscopic Parameters vs. Mechanical Properties of Precambrian Rocks from the Stockholm Region, Sweden*.

Miskovsky, K., Duarte, M. T., Kou, S. Q., and Lindqvist, P. A. (2004). Influence of the Mineralogical Composition and Textural Properties on the Quality of Coarse Aggregates. *Journal of Materials Engineering and Performance, 13*, 144–150. https://doi.org/10.1361/10599490418334

Möller, C. (1998). Decompressed eclogites in the Sveconorwegian (-Grenvillian) orogen of SW Sweden: petrology and tectonic implications. *Journal of Metamorphic Geology, 16*, 641–656. https://doi.org/10.1111/j.1525-1314.1998.00160.x

Möller, C., and Söderlund, U. (1997). Age constraints on the regional deformation within the eastern segment, S. Sweden: Late sveconorwegian granite dyke intrusion and metamorphic-deformational relations. *GFF, 119*(1), 1–12. https://doi.org/10.1080/11035899709546447

Möller, C., Andersson, J., Lundqvist, I., and Hellström, F. (2007). Linking deformation, migmatite formation and zircon U-Pb geochronology in polymetamorphic orthogneisses, Sveconor-

wegian Province, Sweden. *Journal of Metamorphic Geology, 25*(7), 727–750. https://doi.org/10.1111/j.1525-1314.2007.00726.x

Möller, C., Andersson, J., Dyck, B., and Antal Lundin, I. (2015). Exhumation of an eclogite terrane as a hot migmatitic nappe, Sveconorwegian orogen. *Lithos, 226*, 147–168. https://doi.org/10.1016/J.LITHOS.2014.12.013

Möller, C., and Andersson, J. (2018). Metamorphic zoning and behaviour of an underthrusting continental plate. *Journal of Metamorphic Geology, 36*(5), 567–589. https://doi.org/10.1111/jmg.12304

Mortensen, G., and Göransson, M. (2018). *Bergkvalitet Skåne–beskrivning till bergkvalitetskartor över delar av Söderåsen, Kristianstadsområdet, Linderödsåsen och Romeleåsen.* https://doi.org/ISSN 1652-8336.

Nickolsky, M. S., and Yudintsev, S. V. (2021). Electron Backscattered Diffraction for the Study of Matrices for Immobilization of Actinides Composed of the Murataite-Type Phases. *Crystallography Reports, 66*(1), 130–141. https://doi.org/10.1134/S1063774521010090

Passchier, C. W., and Trouw, R. A. J. (2005). *Microtectonics.* (Second ed.). Springer. https://doi.org/10.1007/3-540-29359-0

Petersson, A., Scherstén, A., Bingen, B., Gerdes, A., and Whitehouse, M. J. (2015a). Mesoproterozoic continental growth: U–Pb–Hf–O zircon record in the Idefjorden Terrane, Sveconorwegian Orogen. *Precambrian Research, 261*, 75–95. https://doi.org/10.1016/J.PRECAMRES.2015.02.006

Petersson, A., Scherstén, A., Andersson, J., and Möller, C. (2015b). Zircon U–Pb and Hf – isotopes from the eastern part of the Sveconorwegian Orogen, SW Sweden: implications for the growth of Fennoscandia. *Geological Society, London, Special Publications, 389*(1), 281–303. https://doi.org/10.1144/SP389.2

Piñán-Llamas, A., Andersson, J., Möller, C., Johansson, L., and Hansen, E. (2015). Polyphasal foreland-vergent deformation in a deep section of the 1Ga Sveconorwegian orogen. *Precambrian Research, 265*, 121–149. https://doi.org/10.1016/j.precamres.2015.05.009

Putnis, A., and John, T. (2010). Replacement Processes in the Earth's Crust. *Elements, 6*, 159–164. https://doi.org/10.2113/gselements.6.3.159

Rasband, W. . (1997). ImageJ. In *U. S. National Institutes of Health, Bethesda, Maryland, USA*. U. S. National Institutes of Health. https://doi.org/imagej.nih.gov/ij/

Reed, S. J. B. (1993). *Electron Microprobe Analysis and Scanning Electron Microscopy in Geology.* Cambridge University Press. https://doi.org/http://dx.doi.org/10.1017/CBO9780511610561

Ripa, M., and Stephens, M. B. (2020). Siliciclastic sedimentation in a foreland basin to the Sveconorwegian orogen and dolerites (0.98-0.95 Ga) related to intracratonic rifting. In M. B. Stephens and J. Bergman-Weihed (Eds.), *Sweden: Lithotectonic Framework, Tectonic Evolution and Mineral Resources* (Vol. 50, pp. 325–333). Geological Society, London. https://doi.org/10.1144/M50-2017-6

Rodhe, A. (1992). Terminology and ideas regarding the Protogine Zone in southern Sweden. *GFF, 114*(3), 360–365. https://doi.org/10.1080/11035899209454808

Sajid, M., Coggan, J., Arif, M., Andersen, J., and Rollinson, G. (2016). Petrographic features as an effective indicator for the variation in strength of granites. *Engineering Geology, 202*, 44–54. https://doi.org/10.1016/j.enggeo.2016.01.001

Sawyer, E. W. (1999). Criteria for the recognition of partial melting. *Physics and Chemistry of the Earth, Part A: Solid Earth and Geodesy, 24*(3), 269–279. https://doi.org/10.1016/S1464-1895(99)00029-0

Sawyer, E. W. (2008). *Atlas of migmatites.* The Canadian Mineralogist (ed.); Special Pub. NRC Research Press.

Sawyer, E. W., and Brown, M. (2008). *Working with migmatites* (Short Course). Mineralogical Association of Canada. http://www.mineralogicalassociation.ca/doc/toc_SC38.pdf

Sawyer, E. W., Cesare, B., and Brown, M. (2011). When the Continental Crust Melts. *Elements, 7*(4), 229–234. https://doi.org/10.2113/gselements.7.4.229

Schmid, R., Fettes, D., Harte, B., Davis, E., Desmons, J., Meyer-Marsilius, H. J., and Siivola, J. (2004). A systematic nomenclature for met-

amorphic rocks. In *Subcommission on the Systematics of Metamorphic Rocks –SCMR– terminology*.

Schoene, B. (2013). U-Th-Pb Geochronology. In *Treatise on Geochemistry* (Second ed., Vol. 4, pp. 341–378). https://doi.org/10.1016/B978-0-08-095975-7.00310-7

Schwartz, A. J., Kumar, M., Adams, B. L., and Field, D. P. (2009). Electron backscatter diffraction in materials science. Electron Backscatter Diffraction in Materials Science, 1–403. https://doi.org/10.1007/978-0-387-88136-2

Schwindinger, M., Weinberg, R. F., and Clos, F. (2019). Wet or dry? The difficulty of identifying the presence of water during crustal melting. *Journal of Metamorphic Geology, 37*(3), 339–358. https://doi.org/10.1111/jmg.12465

Slagstad, T., Roberts, N. M. W., Marker, M., Røhr, T. S., and Schiellerup, H. (2013). A non-collisional, accretionary Sveconorwegian orogen. *Terra Nova, 25*(1), 30–37. https://doi.org/10.1111/ter.12001

Slagstad, T., Marker, M., Roberts, N. M. W., Saalmann, K., Kirkland, C., Kulakov, E., Ganerød, M., Røhr, T. S., Møkkelgjerd, S. H. H., Granseth, A., and Sørensen, B. E. (2020). The Sveconorwegian orogeny – reamalgamation of the fragmented southwestern margin of Fennoscandia. *Precambrian Research,* 105877. https://doi.org/10.1016/j.precamres.2020.105877

Slagstad, T., Kulakov, E. V., Anderson, M. W., Saalmann, K., Kirkland, C. L., Henderson, I. H. C., and Ganerød, M. (2023). Was Baltica part of Rodinia? *Terra Nova, 00*, 1–7. https://doi.org/10.1111/TER.12640

Söderlund, P., Söderlund, U., Möller, C., Gorbatschev, R., and Rodhe, A. (2004). Petrology and ion microprobe U-Pb chronology applied to a metabasic intrusion in southern Sweden: A study on zircon formation during metamorphism and deformation. *Tectonics, 23*, TC5005. https://doi.org/10.1029/2003TC001498

Söderlund, U., Jarl, L. G., Persson, P. O., Stephens, M. B. and Wahlgren, C. H. (1999) Protolith ages and timing of deformation in the eastern, marginal part of the Sveconorwegian orogen, southwestern Sweden. *Precambrian Research, 94*(1–2), 29–48. https://doi.org/10.1016/S0301-9268(98)00104-1.

Söderlund, U., Möller, C., Andersson, J., Johansson, L., and Whitehouse, M. J. (2002). Zircon geochronology in polymetamorphic gneisses in the Sveconorwegian orogen, SW Sweden: ion microprobe evidence for 1.46–1.42 and 0.98–0.96 Ga reworking. *Precambrian Research, 113*(3–4), 193–225. https://doi.org/10.1016/S0301-9268(01)00206-6

Söderlund, U., Isachsen, C. E., Bylund, G., Heaman, L. M., Patchett, P. J., Vervoort, J. D., and Andersson, U. B. (2005). U-Pb baddeleyite ages and Hf, Nd isotope chemistry constraining repeated mafic magmatism in the Fennoscandian Shield from 1.6 to 0.9 Ga. *Contributions to Mineralogy and Petrology, 150*(2), 174–194. https://doi.org/10.1007/s00410-005-0011-1

Söderlund, U., and Ask, R. (2006). Mesoproterozoic bimodal magmatism along the protogine zone, S Sweden: Three magmatic pulses at 1.56, 1.22 and 1.205 Ga, and regional implications. *GFF, 128*(4), 303–310. https://doi.org/10.1080/11035890601284303

Song, S., and Cao, Y. (2021). Textures and Structures of Metamorphic Rocks. In *Encyclopedia of Geology* (pp. 375–388). Academic Press. https://doi.org/10.1016/B978-0-08-102908-4.00052-7

Stacey, J. S., and Kramers, J. D. (1975). Approximation of terrestrial lead isotope evolution by a two-stage model. *Earth and Planetary Science Letters, 26*(2), 207–221. https://doi.org/10.1016/0012-821X(75)90088-6

Stephens, M. B., Wahlgren, C. H., Weijermars, R., and Cruden, A. R. (1996). Left-lateral transpressive deformation and its tectonic implications, Sveconorwegian orogen, Baltic Shield, southwestern Sweden. *Precambrian Research, 79*(3–4), 261–279. https://doi.org/10.1016/0301-9268(95)00097-6

Stephens, M. B., and Wahlgren, C.H. (2020a). Accretionary orogens reworked in an overriding plate setting during protracted continent–continent collision, Sveconorwegian orogen, southwestern Sweden. In M. B. Stephens and J. Bergman-Weihed (Eds.), *Sweden: Lithotectonic Framework, Tectonic Evolution and Mineral Resources. Geological Society, London, Memoirs* (Vol. 50, Issue 1, pp. 435–448). Geological Society of London. https://doi.org/10.1144/M50-2018-83

Stephens, M. B., and Wahlgren, C.-H. (2020b). Polyphase (1.9–1.8, 1.5–1.4 and 1.0–0.9 Ga) deformation and metamorphism of Proterozoic (1.9–1.2 Ga) continental crust, Eastern Segment, Sveconorwegian orogen. In M. B. Stephens and J. Bergman-Weihed (Eds.), *Sweden: Lithotectonic Framework, Tectonic Evolution and Mineral Resources. Geological Society, London, Memoirs* (Vol. 50, Issue 1, pp. 351–396). Geological Society of London. https://doi.org/10.1144/M50-2018-57

Stuart, C. A., Daczko, N. R., and Piazolo, S. (2017). Local partial melting of the lower crust triggered by hydration through melt-rock interaction: an example from Fiordland, New Zealand. *Journal of Metamorphic Geology, 35*(2), 213–230. https://doi.org/10.1111/jmg.12229

Sveriges geologiska undersökning SGU-rapport (2015) 39 *Resurseffektivisering och minskade transporter –förslag till hur insamling av produktionsuppgifter från entreprenadberg kan utformas. Dnr 317-1681/2013*

Svensk Standard (2010) SS-EN 1097-1. *Ballast – Mekaniska och fysikaliska egenskaper – Del 1: Bestämning av nötningsmotstånd (Micro-Deval)*. Swedish Standards Institute, Sweden.

Svensk Standard (2010) SS-EN 1097-2. *Ballast – Mekaniska och fysikaliska egenskaper – Del 2: Bestämning av motstånd mot sönderdelning*. Swedish Standards Institute, Sweden.

Trotta, R. P., Barroso, E. V., and da Motta, L. M. G. (2021). Migmatitic gneiss aggregates: Compositional, mechanical, and morphological responses to innate heterogeneity. *Engineering Geology, 283*, 106002. https://doi.org/10.1016/J.ENGGEO.2021.106002

Tual, L., Pinan-Llamas, A., Möller, C., Piñán-Llamas, A., and Möller, C. (2015). High-temperature deformation in the basal shear zone of an eclogite-bearing fold nappe, Sveconorwegian orogen, Sweden. Precambrian Research, 265, 104–120. https://doi.org/10.1016/j.precamres.2015.05.007

Tual, L., Pitra, P., and Möller, C. (2017). P-T evolution of Precambrian eclogite in the Sveconorwegian orogen, SW Sweden. *Journal of Metamorphic Geology, 35*(5), 493–515. https://doi.org/10.1111/jmg.12242

Tuğrul, A., and Zarif, I. H. (1999). Correlation of mineralogical and textural characteristics with engineering properties of selected granitic rocks from Turkey. *Engineering Geology, 51*(4), 303–317. https://doi.org/10.1016/S0013-7952(98)00071-4

Ulmius, J., Andersson, J., and Möller, C. (2015). Hallandian 1.45 Ga high-temperature metamorphism in Baltica: P-T evolution and SIMS U-Pb zircon ages of aluminous gneisses, SW Sweden. *Precambrian Research, 265*, 10–39. https://doi.org/10.1016/j.precamres.2015.04.004

Ulmius, J., Möller, C., Page, L., Johansson, L., and Ganerød, M. (2018). The eastern boundary of Sveconorwegian reworking in the Baltic Shield, defined by 40Ar/39Ar geochronology across the southernmost Sveconorwegian Province. *Precambrian Research, 307*, 201–217. https://doi.org/10.1016/j.precamres.2018.01.008

Vernon, R. H. (2004). *A practical guide of microstructures*. Cambridge University Press. https://doi.org/https://doi.org/10.1017/9781108654609

Vernon, R. H. (2011). Microstructures of melt-bearing regional metamorphic rocks. In D. D. van Reenen, J. D. Kramers, S. McCourt, and L. L. Perchuk (Eds.), *Origin and Evolution of Precambrian High-Grade Gneiss Terranes, with Special Emphasis on the Limpopo Complex of Southern Africa: Geological Society of America Memoir* (Vol. 207, pp. 1–11). The Geological Society of America. https://doi.org/10.1130/2011.1207(01)

Viola, G., and Henderson, I. C. (2010). Inclined transpression at the toe of an arcuate thrust: an example from the Precambrian "Mylonite Zone" of the Sveconorwegian orogen. In R. D. Law, R. W. H. Butler, R. E. Holdsworth, M. Krabbendam, and R. A. Strachan (Eds.), *Continental Tectonics and Mountain Building: The Legacy of Peach and Horne* (Vol. 335, pp. 715–737). Geological Society, London, Special Publications. https://doi.org/10.1144/SP335.29

Viola, G., Henderson, I. H. C., Bingen, B., and Hendriks, B. W. H. (2011). The Grenvillian–Sveconorwegian orogeny in Fennoscandia: Back-thrusting and extensional shearing along the "Mylonite Zone." *Precambrian Research, 189*(3–4), 368–388. https://doi.org/10.1016/J.PRECAMRES.2011.06.005

Wahlgren, C. H., Cruden, A. R., and Stephens, M. B. (1994). Kinematics of a major fan-like structure in the eastern part of the Sveconorwegian orogen, Baltic Shield, south-central Sweden. *Precambrian Research, 70*(1–2), 67–91. https://doi.org/10.1016/0301-9268(94)90021-3

Wang, X. D., and Lindh, A. (1996). Temperature-pressure Investigation of the Southern Part of the Southwest Swedish Granulite Region. *European Journal of Mineralogy, 8*(1), 51–68. https://doi.org/10.1127/ejm/8/1/0051

Weinberg, R. F., and Hasalová, P. (2015). Water-fluxed melting of the continental crust: A review. *Lithos, 212–215*, 158–188. https://doi.org/10.1016/j.lithos.2014.08.021

Weller, O. M., Mottram, C. M., St-Onge, M. R., Möller, C., Strachan, R., Rivers, T., and Copley, A. (2021). The metamorphic and magmatic record of collisional orogens. *Nature Reviews Earth and Environment, 2*, 781–799. https://doi.org/10.1038/s43017-021-00218-z

Whitehouse, M. J., Claesson, S., Sunde, T., and Vestin, J. (1997). Ion microprobe U-Pb zircon geochronology and correlation of Archaean gneisses from the Lewisian Complex of Gruinard Bay, northwestern Scotland. *Geochimica et Cosmochimica Acta, 61*(20), 4429–4438. https://doi.org/10.1016/S0016-7037(97)00251-2

Wik, N. G., Andersson, J., Bergström, U., Claeson, D., Juhojuntti, N., Kero, L., Lundqvist, L., Möller, C., Sukotjo, S., and Wikman, H. (2006). *Beskrivning till regional berggrundskarta över Jönköpings län. K,61*.

Wilkinson, A. J., and Britton, T. B. (2012). Strains, planes, and EBSD in materials science. *Materials Today, 15*(9), 366–376. https://doi.org/10.1016/S1369-7021(12)70163-3